

FRACTURE OF GYPSUM PLASTERS AND CEMENT MORTARS BY DYNAMIC LOADING

Dr. Charles W. Martin

Melpar, Inc.
Falls Church, Virginia
Contract AF29(601)-6420

Code 1

CLEARINGHOUSE FOR FEDERAL SCIENTIFIC AND TECHNICAL INFORMATION			
Hardcopy	Microfilm		
\$ 3.00	\$ 0.75	80	BOT
ADDITIONAL COPY			

TECHNICAL REPORT NO. AFWL-TR-65-140

December 1965

AIR FORCE WEAPONS LABORATORY
Research and Technology Division
Air Force Systems Command
Kirtland Air Force Base
New Mexico



AD625428

AFWL-TR-65-140

FRACTURE OF GYPSUM PLASTERS AND CEMENT
MORTARS BY DYNAMIC LOADING

Dr. Charles W. Martin

Melpar, Inc.
Falls Church, Virginia
Contract AF29(601)-6420

TECHNICAL REPORT NO. AFWL-TR-65-140

Distribution of this document is unlimited.
--

AFWL-TR-65-140

Research and Technology Division
AIR FORCE WEAPONS LABORATORY
Air Force Systems Command
Kirtland Air Force Base
New Mexico

When U. S. Government drawings, specifications, or other data are used for any purpose other than a definitely related Government procurement operation, the Government thereby incurs no responsibility nor any obligation whatsoever, and the fact that the Government may have formulated, furnished, or in any way supplied the said drawings, specifications, or other data, is not to be regarded by implication or otherwise, as in any manner licensing the holder or any other person or corporation, or conveying any rights or permission to manufacture, use, or sell any patented invention that may in any way be related thereto.

This report is made available for study with the understanding that proprietary interests in and relating thereto will not be impaired. In case of apparent conflict or any other questions between the Government's rights and those of others, notify the Judge Advocate, Air Force Systems Command, Andrews Air Force Base, Washington, D. C. 20331.

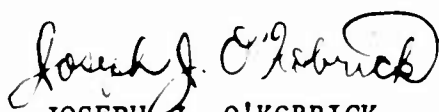
Distribution of this document is unlimited.


FOREWORD

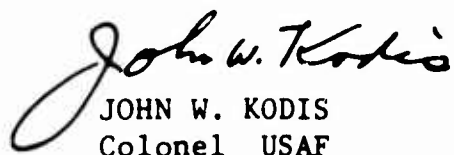
This report was prepared by Melpar, Inc., Falls Church, Virginia, under Contract AF29(601)-6420. The research was performed under Program Element 7.60.06.01.D, Project 5710, Subtask 13.144, and funded by Defense Atomic Support Agency (DASA). Inclusive dates of research are 8 June 1964 to 1 July 1965. This report was submitted for publication on 18 November 1965 by the AFWL Project Officer, Captain Joseph J. O'Kobrick (WLDC).

The principal investigator at Melpar was Dr. Charles W. Martin, and the Project Monitor for the AFWL was Captain Thomas E. O'Brien (WLDC).

This report has been reviewed and is approved.


JOSEPH J. O'KOBICK
Captain USAF
Project Officer


ROBERT E. CRAWFORD
Major USAF
Deputy Chief
Civil Engineering Branch


JOHN W. KODIS
Colonel USAF
Chief, Development Division

ABSTRACT

An experimental study was made of influence of strain magnitude and strain duration on dynamic fracture in uniaxial tension of low-strength gypsum plaster, high-strength gypsum plaster, high early strength portland cement mortar, and ordinary portland cement mortar. Dynamic test specimens were circular cylindrical bars with diameters ranging from 0.9 to 1.2 inches and lengths ranging from 18 to 58 inches. Static test specimens 2 inches long were cut from the long bars. A special loading device, designed and constructed by Melpar, generated a compressive pulse by longitudinal impact of two metal bars and applied the pulse to one end of the dynamic test specimens. The compressive pulse was reflected at the free end of specimens as a tensile pulse and caused fracture in tension at a section near the middle.

Time from zero strain to maximum tensile strain varied from 10 to 35 microseconds, and total duration of tensile strain varied from 20 to 430 microseconds with few exceptions. All materials withstood tensile strains two to three times the static fracture strain for short periods. The straining time required to cause fracture varied with strain magnitude.

CONTENTS

<u>Section</u>	<u>Page</u>
1. INTRODUCTION	1
2. CONCEPT OF EXPERIMENTS	5
3. EXPERIMENTAL METHODS	9
a. Method for Casting Dynamic Test Specimens from Low-Strength Gypsum Plaster	9
b. Method for Casting Dynamic Test Specimens from High-Strength Gypsum Plaster	11
c. Method for Casting Dynamic Test Specimens from Portland Cement Mortars	15
d. Method for Determining Static Tensile Strength and Density	18
e. Method for Cutting Test Specimens and Applying Gages and Conductive Strips	20
f. Method for Determining Moisture Content at Time of Dynamic Test	24
g. Method for Dynamic Fracture Testing	25
4. RESULTS	43
a. Ultracal 60 Series 1	50
b. Ultracal 60 Series 2	53
c. Hydrostone	54
d. Portland Cement Mortars	54
e. Applications	64
5. CONCLUSIONS	71
REFERENCES	73
DISTRIBUTION	75

LIST OF FIGURES

<u>Figure</u>		<u>Page</u>
1.	Schematic of Loading Arrangement and Idealized Loading Conditions	6
2.	Schematic of Apparatus for Mixing Hydrostone	12
3.	Equipment for Mixing High Strength Gypsum Plaster	13
4.	Equipment for Mixing Portland Cement Mortars	16
5.	Equipment for Cutting Test Specimens	19
6.	Mortar Dynamic Test Specimens Before and After Testing	21
7.	Loading Apparatus	27
8.	Details of Anvil and Striker Bars	29
9.	End View of Loading Apparatus	30
10.	Photograph of Loading Apparatus Outside Darkroom	31
11.	Photograph of Loading Apparatus Inside Darkroom	32
12.	First Test Equipment Block Diagram	33
13.	Sketch of Data from First Series of Tests with Notation	35
14.	Sketch of Measurements on Photograph of Specimen with Notation	36
15.	Second Test Equipment Block Diagram	37
16.	Circuit Diagrams	38
17.	Photograph of Recording Equipment	39
18.	Sketch of Data from Tests Excepting First Series	40

LIST OF FIGURES (Cont.)

<u>Figure</u>		<u>Page</u>
19.	Photograph of Original Data from Tests Excepting First Series	41
20.	Strain Magnitude vs. Strain Duration for Ultracal 60, Series 2	47
21.	Strain Magnitude vs. Strain Duration for Hydrostone	48
22.	Strain Magnitude vs. Strain Duration for High Early Strength Mortar	49
23.	Strain Magnitude vs. Strain Duration for Ordinary Mortar	63

LIST OF TABLES

<u>Table</u>		<u>Page</u>
I	Location of Strain Gages and Conductive Strips	23
II	Properties of Materials	45
III	Data from Dynamic Tests of Ultracal 60, Series 1	51
IV	Data from Dynamic Tests of Ultracal 60, Series 2	55
V	Data from Dynamic Test of Hydrostone	57
VI	Data from Dynamic Tests of High Early Strength Portland Cement Mortar	65
VII	Data from Dynamic Tests of Ordinary Portland Cement Mortar	67
VIII	Energy Associated with Fracture of Ultracal 60	69

LIST OF SYMBOLS

d_1	Distance from free end to strain gage
d_2	Distance from free end to first fracture
d_3	Distance from free end to section where tensile stress first reaches its maximum
D	Diameter of static test specimen
c	Propagation velocity of pulse
$K =$	$\int_0^{t_4} \left[\frac{\epsilon - \epsilon_s}{\epsilon_s} \right] dt$
L	Length of static specimen
M_1	Momentum/unit area in incident compressive pulse (See figure 14.)
M_2	Momentum/unit area in fragments between first crack and free end (using conductive strip data) (See figure 14.)
M_3	Momentum/unit area in fragments between first crack and free end (using photograph data) (See figure 14.)
M_4	Momentum/unit area in reflected tensile pulse at strain gage. (See figure 14.)
P	Load applied to static test specimen
S	Static tensile strength
t	Time
t_r	Rise time of a pulse
t_1	Interval between arrivals of compressive pulse and tensile pulse (See figure 13.)
t_2	Duration of compressive phase at strain gage minus fall time (See figure 13)

LIST OF SYMBOLS (Cont.)

t_3	Duration of compressive phase at strain gage (See figure 13.)
t_4	Duration of tensile phase at strain gage (See figure 13.)
t_5	Interval between first compressive strain at gage and break of conductive strip (See figure 13.)
t_6	Interval between break of conductive strip and firing first strobe light (See figure 13.)
t_7	Interval between firing two strobe lights (See figure 13.)
t_8	Duration of maximum strain (See figure 13.)
t_9	Interval from zero strain to maximum tensile strain (See figure 18.)
$T =$	Interval between arrival of compressive pulse and first occurrence of tension (See figure 13.)
ϵ	Strain
ϵ_1	Magnitude of incident compressive strain pulse
ϵ_2	Magnitude of reflected tensile strain pulse
ϵ_s	Static fracture strain
$\rho =$	Density = mass per unit volume

SECTION I

INTRODUCTION

In this investigation, experimental data have been generated which provide an improved understanding of stress-strain time conditions necessary to cause tensile fracture of gypsum plasters and concrete mortars when the time of applying load is in the order of 20 microseconds. It is hoped that research of this nature will eventually produce a simple mathematical statement of conditions necessary for fracture of a broad class of rock-like materials. Also, it is hoped that a simple test will be developed for determining a property which is a measure of resistance to fracture of these materials by very rapid tensile loading.

Dynamic tensile fractures are thought to occur in many important practical cases, including the collapse of subsurface tunnels, cratering, and percussion drilling. It is believed that dynamic fracture in tension is a very important part of the complex phenomena of behavior of rock under explosive or impact loading. Improved understanding of the phenomenon has important application to model prediction of fracture. In addition, improved understanding of dynamic tensile fracture may lead to significant improvements in efficiency in drilling, blasting, and demolition and to better design criteria for blast-resistant structures.

The basic reason usually advanced for the great importance of tensile fracture, as compared to compressive or shear fracture, is that the ratio of compressive strength to tensile strength of rocks¹ varies from 10 to 20. Since tensile strengths are so much lower than compressive strengths, rocks will transmit intense compression stress pulses without damage; but when tensile stress is produced by some means, such as reflection at a free surface, the rock is readily fractured.

There is considerable evidence that fracture under rapidly applied loading cannot be predicted by specifying a state of stress or strain. Specification of the conditions causing fracture must also include time.

Dynamic fracture in tension for loading durations in the range of 20 to 500 microseconds is an important part of the complex phenomena of behavior of rock under blast or impact loading. Load durations in this range have been observed in instrumented laboratory scale model experiments^{2,3} and in field tests involving several pounds of explosive.^{4,5,6}

Several investigators have discussed the importance of tensile fracture in general^{7,8} and its particular importance in rock blasting.^{5,9,10}

Reichmuth¹ concluded that the initial fracture and subsequent fractures producing chips in percussion drilling were tensile fractures. He also noted that the force required to produce a given penetration of a bit was higher for dynamic loading than for static loading.

Martin and Murphy¹¹ performed dynamic tensile fracture experiments with gypsum plaster bars. Their investigation was prompted by the following observations:

a. Numerous observations^{4,6} of strain wave propagation in rock show "cube root scaling" to be valid over a considerable range of charge size. "Cube root scaling" means scaling all linear dimensions (i.e., travel distance) by the cube root of the charge size. If the condition of fracture can be specified as a state of stress or strain, dimensional analysis leads to the conclusion that cube root scaling should also be valid for predicting fracture.

b. Data obtained from several sources^{3,8,10} indicated considerable deviation from cube root scaling in fracture due to explosions.

c. Reported values of dynamic tensile fracture stresses^{4,5,7,10} are invariably higher than static fracture stresses for the same materials. However, reported ratios of dynamic-to-static fracture stresses vary widely.

Among the conclusions reached by Martin and Murphy,¹¹ the following are considered especially significant:

a. The time required to complete fracture of plaster is significant, and it varies with the level of stress. It follows that direct application of cube root scaling is not valid in the range of load durations considered.

b. The condition of dynamic fracture of plaster cannot be specified only in terms of stress or strain.

c. There should exist some function of stress such that the time integral of the function of stress to completion of fracture is a constant characteristic of the material. A form of this function applicable to plaster was proposed.

In the present investigation, a considerable amount of experimental data has been obtained for high-strength gypsum plaster, low-strength gypsum plaster, high early strength portland cement mortar, and ordinary portland cement mortar. Time from zero strain to maximum tensile strain in specimens was between about 10 and 35 microseconds in most cases.

Duration of straining varied from about 20 to 430 microseconds -- more than twice the range of load durations investigated by Martin and Murphy.¹¹ A total of 321 dynamic tests was performed in addition to 256 static tensile strength tests and numerous preliminary tests. A number of innovations in instrumentation were made including a simple method of photographing the specimens at two stages during dynamic fracture.

A simple mathematical statement of conditions necessary for fracture of a broad class of rock-like materials, and a simple test for evaluating resistance to dynamic fracture have not yet been evolved. However, it is felt that significant progress has been made toward these objectives.

BLANK PAGE

SECTION 2

CONCEPT OF EXPERIMENTS

In these experiments it was desired that specimens be brought from a state of either compression or zero strain to a state of high tensile strain in the minimum possible time, and held at this high level of strain until fracture was completed.

It is thought that cracks in rock-like materials originate at flaws or in microcracks in the material and that they grow whenever the stress or strain exceeds a value called the static tensile strength. Crack growth is thought to start slowly, to accelerate, and finally to reach an appreciable fraction of the speed of sound in the material. If this is true, the vast majority of area of the specimen is fractured in a very small percentage of the time in which the material has been under load. Propagation of stress pulses in the specimen would be little affected by fracture until crack propagation velocity reached a high value, and then fracture would be completed at a very high rate and in a very short time.

When rock-like materials are loaded by explosion or impact as in blasting, demolition, or percussion drilling, the duration of tensile stressing may be comparable to or less than the time required for crack growth to reach a high velocity. Consequently, it is necessary to investigate the variation of fracture time with intensity of straining in order to predict whether rock-like materials will be fractured by stress pulses of short duration.

A schematic sketch of the loading method, idealized plots of strain vs. time, and idealized plots of strain vs. distance are shown in figure 1. A strain pulse is generated by longitudinal impact of a flat-ended metal bar (referred to as the striker) on another flat-ended metal bar (referred to as the anvil). The pulse propagates down the anvil to the joint between anvil and specimen. At this joint, part of the energy of the pulse is reflected and part transmitted into the specimen. The incident compressive pulse propagates to the end of the specimen and is reflected as a tensile pulse. When the head of the reflected tensile pulse passes the tail of the incident compressive pulse, a section in the middle of the specimen is subjected to tension, which will cause it to fracture if the tensile pulse is sufficiently intense and prolonged.

Propagation of pulses in cylindrical bars has been discussed by a number of authors, for example, Timoshenko¹² and Kolsky.¹³ Two longitudinally impacting bars will remain in contact until the pulse has traveled to the free

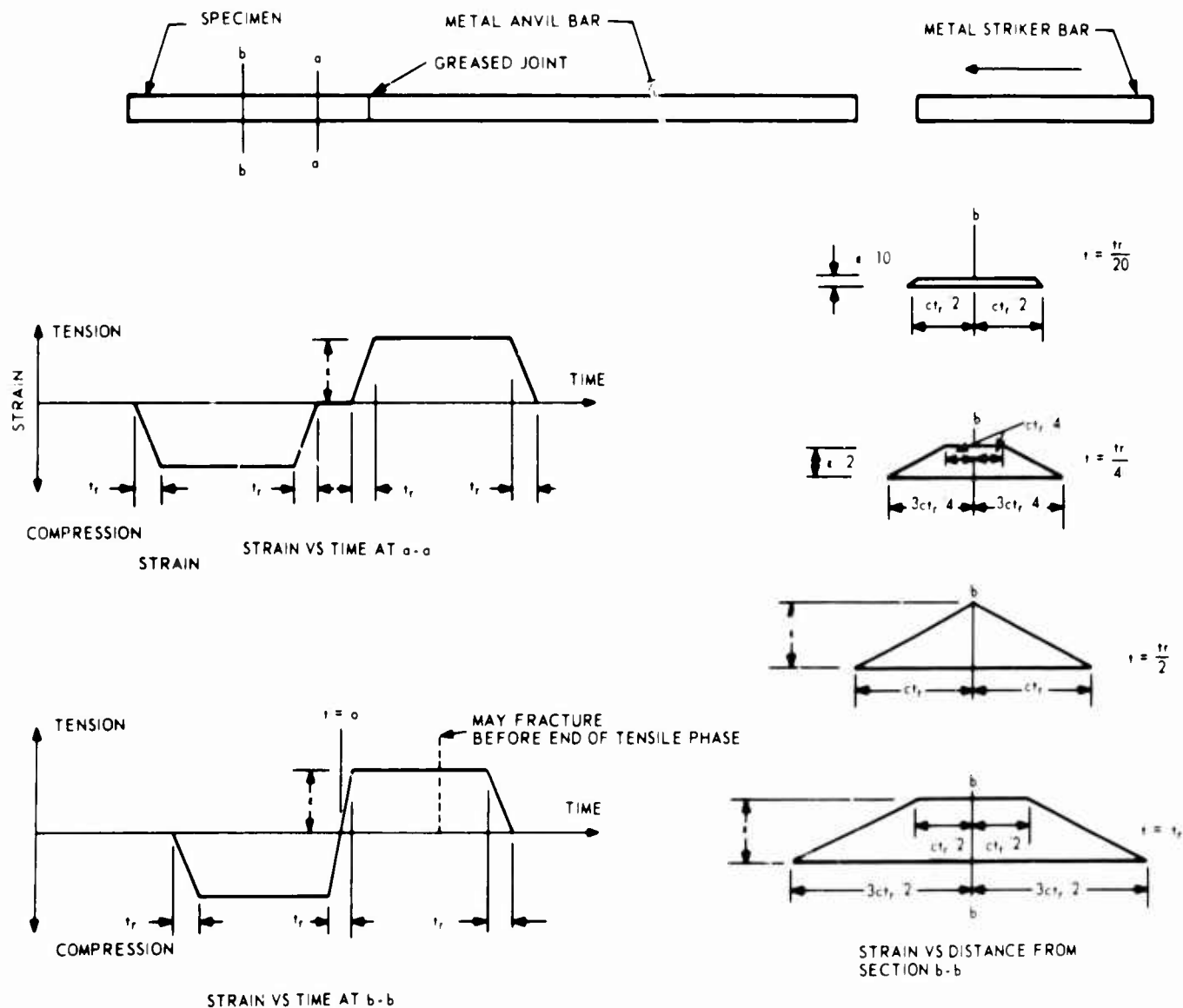


Figure 1. Schematic of Loading Arrangement and Idealized Loading Conditions

end of the shorter bar and back to the surface of contact. Consequently, pulse duration is determined by length of the striker bar and is equal to twice the length of the striker divided by the pulse velocity in the striker. Intensity of the pulse in the metal bars is proportional to velocity of impact. The ratio of stress in the specimen to stress in the anvil depends on the acoustic impedance (density multiplied by pulse propagation velocity) of the two materials.

To avoid undesirable effects from reflection of pulses, it is necessary that the anvil be at least twice as long as the striker bar. Also, the specimen must be at least as long as the physical length of the strain pulse in the specimen, e.g., specimen length must be greater than pulse duration multiplied by pulse velocity in the specimen. If these conditions are satisfied,

a section in the middle of the specimen will remain in tension for the entire pulse duration, or until fracture occurs.

The ideal condition for this type of loading is that the strain at some section of the specimen goes instantly from zero to a high value of tension and remains there until fracture occurs. In practice this cannot be exactly achieved.

Pulse duration is limited by length of the specimen and metal bars. For example, the pulse velocity in the steel bars used is 191,000 inches/sec, and a 25-inch long striker generates a pulse with a nominal duration of 262 microseconds. In high early strength portland cement mortar, pulse velocity was 158,785 inches/sec, and, consequently, the minimum specimen length is 41.6 inches if the specimen is to stay in tension for the entire 262 microsecond duration of the pulse generated by a 25-inch-long striker. Duration of loading can be increased only by increasing the lengths of the specimen, striker, and anvil bars. Obviously, there is a practical limit to the length of specimens that can be handled.

Strain cannot go instantly from zero to a high value of tension because of the finite rise time of the pulse. In practice, it is possible to generate pulses which closely approximate those shown in figure 1. At some section, a-a, remote from the free end of the specimen, the strain increases from zero to a high value of compression during the rise time, t_r ; holds constant for a time; and decreases to zero in a time approximately equal to t_r . The pulse propagates to the end of the specimen, is reflected with a change of phase, and the strain pattern is repeated at section a-a but with tensile strains rather than compressive strains.

If the rise time and fall time of the pulse are equal, there will exist some time at which the tail of the compressive pulse coincides with the head of the reflected tensile pulse, and the resultant strain in the specimen is everywhere zero. An instant later, a zone of length ct_r (where c is the pulse propagation velocity) will be subjected to tension. Section b-b in figure 1 is taken to be at the center of this zone which first goes into tension. Note that at section b-b the time from zero strain to maximum tensile strain is only $t_r/2$. Note also that when strain at section b-b first reaches its maximum value, tensile strains of lesser magnitude exist for a distance equal to ct_r on either side of section b-b.

In practice, t_r has a value of very near 20 microseconds in metal bars of 1-inch diameter. In some cases, t_r was larger in the specimens, probably due to an imperfect joint between the anvil bar and specimen.

In actual experiments, the value of t_r in the specimen varied from about 20 to 50 microseconds, and c varied from about 112,500 to 158,800 inches/sec, so that ct_r varied from 2.3 to 8.0 inches for various materials and test conditions.

A good picture of the loading condition in the specimens is given by the sketch of strain vs. time at section b-b and strain vs. distance from section b-b at various times as shown in figure 1.

SECTION 3

EXPERIMENTAL METHODS

a. Method for Casting Dynamic Test Specimens from Low-strength Gypsum Plaster

(1) Scope

This method covers the materials, mechanical mixing, molds, placement in molds, and curing of low-strength plaster bars for dynamic fracture tests.

(2) Apparatus

(a) Scales: The scale used in weighing materials for plaster mixes was an Ohaus model 1119 having a capacity of 20 kg and a least-scale division of 1 g.

(b) Specimen Molds: Specimen molds were made from 1-inch schedule 80 polyvinyl chloride pipe. Pipe was cut in 40-inch lengths, and lengths with bends or imperfections were discarded. The select 40-inch lengths were sliced lengthwise down one side so that they could be wedged open and the specimen slid out of the mold. A T-shaped gasket was inserted in the slot, and the mold clamped together with screw-type hose clamps at 3-inch intervals, so that the mold was water tight. One end of the mold was closed by a rubber stopper. The inside diameter of the assembled mold was about 0.95 inch. A rack was constructed to hold the molds in a nearly vertical position during placing of the plaster mixture.

(c) Mixing Apparatus: The mixing container was a rectangular polyethylene pan about 11 by 13 by 6 inches deep. Plaster was sifted into the mixing pan with a sieve having a rotating blade above the screen. Mixing was done by hand with a rectangular steel trowel.

(3) Temperature and Humidity

(a) Temperature: Temperature of the air in the work area varied from about 71 to 81 degrees F.

(b) Humidity: Relative humidity in the work area varied from about 20 to 30 percent.

(4) Materials

(a) Plaster: Plaster used was Ultracal 60 gypsum plaster, manufactured by United States Gypsum Company.

(b) Water: Mixing water was ordinary tap water.

(5) Batch Size

Each batch was made up of the following quantities of materials:

Ultracal 60 plaster -- 3800 g.

Water -- 1482 g.

(6) Mixing

Great care was exercised in keeping mixing equipment clean and free of dried plaster.

Water was placed in the pan and then plaster was sifted over the surface as rapidly as it would sink into the water without building up a dry layer on the surface. Sifting plaster into the water required 17 minutes. After the plaster was added, it was allowed to stand undisturbed for 4 minutes.

Gentle mixing with a rectangular steel trowel was done for 20 minutes. Great care was exercised to avoid splashing or other action that might cause entrapment of air.

(7) Placing in Molds

Polyvinyl chloride forms were thoroughly cleaned by forcing a cheese-cloth pad through the mold with a metal rod. A smooth coat of silicone grease was applied by the same technique after replacing the cleaning cloth with one saturated with grease. Molds were made completely water tight.

Molds were held in a rack with a slight incline from the vertical. The mixture was poured down the side of the mold, with great care to avoid splashing or other action that might entrap air.

(8) Curing

Molds were not moved from the casting position for 30 minutes. Specimens were removed from the molds 4 hours after casting. Molds were spread and wedged apart so that specimens would slide out without being forced. Specimens were pushed out with a rod, never pulled out.

After removal from forms, specimens were placed in a rack and air dried until tested.

b. Method for Casting Dynamic Test Specimen from High-Strength Gypsum Plaster

(1) Scope

This method covers the materials, mechanical mixing, molds, placement in molds and curing of high-strength plaster bars for dynamic fracture tests.

(2) Apparatus

(a) Scales: The scale used in weighing materials was the same as previously described for low strength gypsum plaster.

(b) Specimen Molds: Specimen molds were of similar construction to those used for low-strength gypsum plaster. The only variations were greater length (60 inches) for some molds and the widening of the slot at one end of the mold to permit the pouring of the plaster mixture into the molds. The rack for holding these molds was of such construction to hold the molds in a nearly horizontal position.

(c) Mixing Apparatus: A unique apparatus was constructed for degassing water and combining plaster with water at a low pressure -- just above the vapor pressure of water. The apparatus is shown schematically in figure 2, and a photograph is shown in figure 3.

(3) Mixing Procedure

Water and plaster were weighed and placed in their respective flasks. The vacuum pump was connected through the filter and moisture trap to the water flask. The system was evacuated until air bubbles ceased to rise to the surface of the water. After completion of degassing, vacuum was slowly released. The vacuum pump was then connected through the filter to the flask containing plaster, the pressure was reduced to 0.25 psi, and

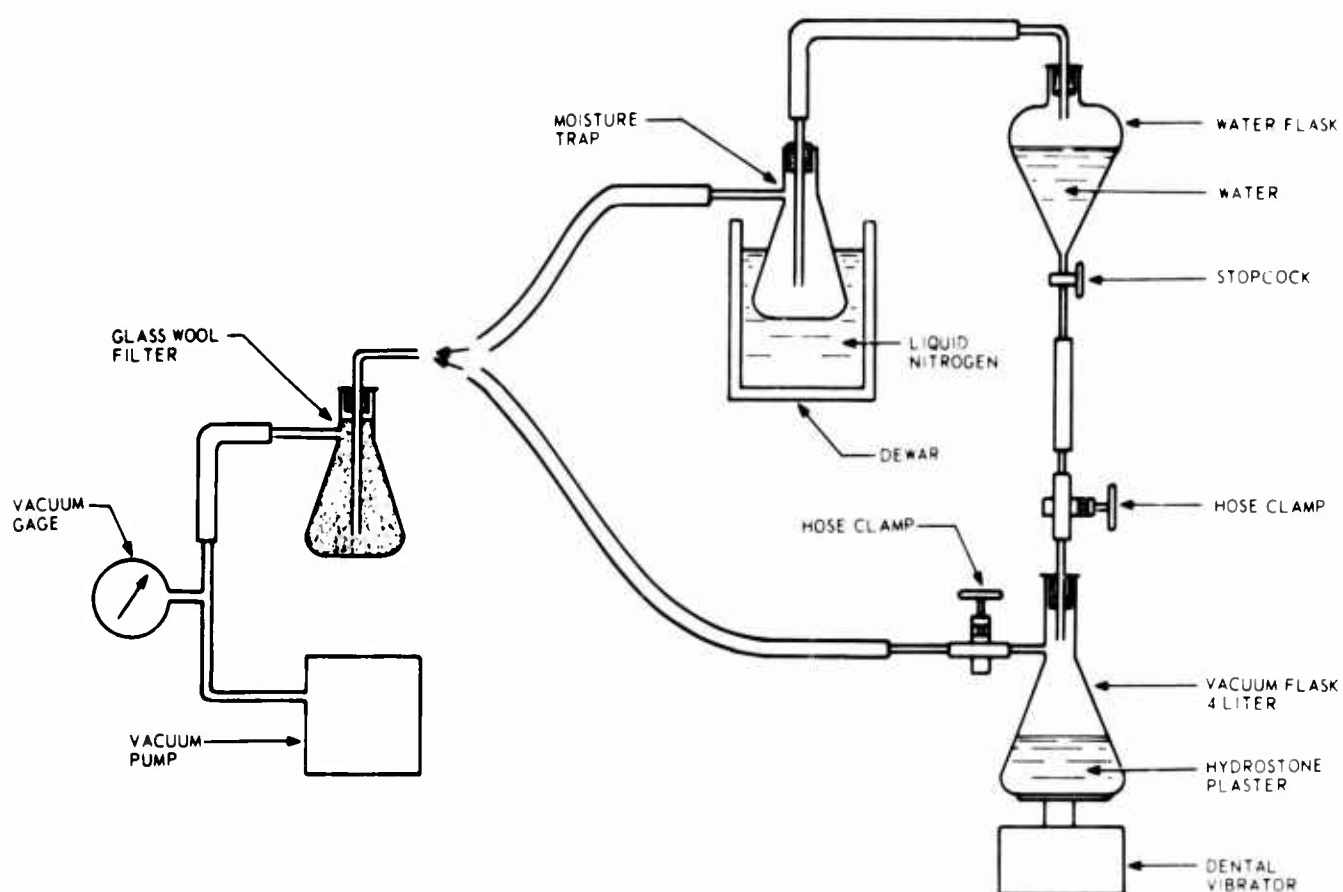


Figure 2. Schematic of Apparatus for Mixing High-Strength Gypsum Plaster

the connection between the pump and plaster flask was closed. The vibrator was operated only during evacuation of the plaster flask. It was a 110-volt, 2.5-amp dental vibrator made by the Buffalo Dental Manufacturing Company. The stopcock between the water flask and the plaster flask was then opened, and water was allowed to run into the plaster flask. A few drops of water were left in the water flask so that a vacuum was maintained in the plaster flask. Injection of water required 1 minute. After injection of water, the clamp on the hose leading to the plaster flask was closed, and the plaster flask was removed from the system.

Mixing was accomplished by vigorously shaking the flask for 11 minutes, after which the vacuum was slowly released, and the mixture was rapidly poured into the molds.

(4) Temperature and Humidity

(a) Temperature: Temperature of the air in the work area varied from about 71 to 81 degrees F.

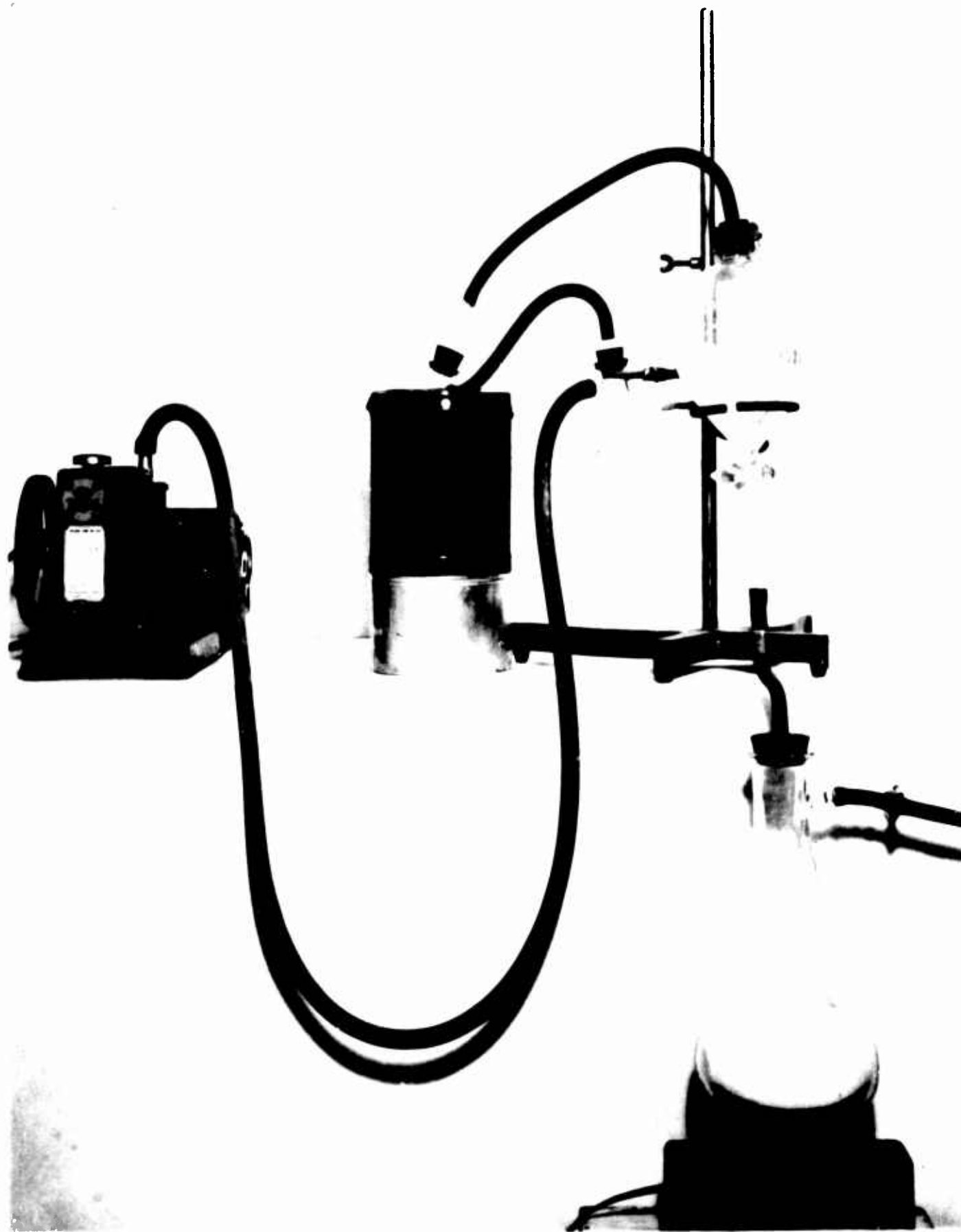


Figure 3. Equipment for Mixing High Strength Gypsum Plaster

(b) Humidity: Relative humidity in the work area varied from about 20 to 30 percent.

(5) Materials

(a) Plaster: Plaster used was Hydrostone gypsum plaster, manufactured by United States Gypsum Company.

(b) Water: Mixing water was ordinary tap water.

(6) Batch Size

Each batch was made up of the following quantities of materials:

Hydrostone plaster -- 2700 g.

Water -- 900 g.

(7) Placing in Molds

Slotted polyvinyl chloride molds were thoroughly cleaned by forcing a cheese-cloth pad through the mold with a metal rod. A smooth coat of silicone grease was applied by the same technique after replacing the cleaning cloth with one saturated with grease.

Molds were held in a rack with a slight incline from the horizontal. Plaster poured through a funnel into an opening at one end flowed down the mold and overflowed through the slot along the top of the mold so that no air was trapped.

(8) Curing

Molds were not moved from the casting position for 30 minutes. Specimens were removed from the molds 4 hours after casting. Molds were spread and wedged apart so that specimens would slide out without being forced. Specimens were pushed out with a rod, never pulled out.

After removal from forms, specimens were placed in a rack and air dried until tested.

c. Method for Casting Dynamic Test Specimens from Portland Cement Mortars

(1) Scope

This method covers the materials, mechanical mixing, molds, placing in molds, and curing of portland cement mortar bars for dynamic fracture tests.

(2) Apparatus

(a) Scales: The scale previously described was used in weighing materials for mortar mixes.

(b) Specimen Molds: Specimen molds were made from 1-1/4-inch, schedule 80 polyvinyl chloride pipe. Pipe was cut in 50-inch lengths, and lengths with bends or surface imperfections were discarded. The select 50-inch pieces were sliced lengthwise, and each half was marked so that it could be matched with its mating half. When assembled, the two halves of the mold were held together by 11 screw-type hose clamps. The bottom of the mold was closed by a rubber stopper. The inside diameter of an assembled mold was about 1.2 inches. Each half of the mold was lubricated with silicone grease before assembly.

(c) Mixer, Bowl, and Paddle: The mixer was a Hobart model C-100, electrically driven, 3-speed mechanical mixer shown in figure 4. This mixer is similar to that described in ASTM designation C305¹⁴ but is larger, the bowl diameter being about 10 inches and the bowl height about 9 inches.

(d) Tamper: The tamper was an aluminum bar of 50 inches in length and 1.00 inch in diameter. A thin rubber cap covered the end.

(3) Temperature and Humidity

(a) Temperature: Temperature of the air in the work area varied from about 71 to 81 degrees F.

(b) Humidity: Relative humidity in the work area varied from about 20 to 30 percent.

(4) Materials

(a) Cement: Portland cement was purchased from a local supplier. All specimens in one series were made from a single bag of high-

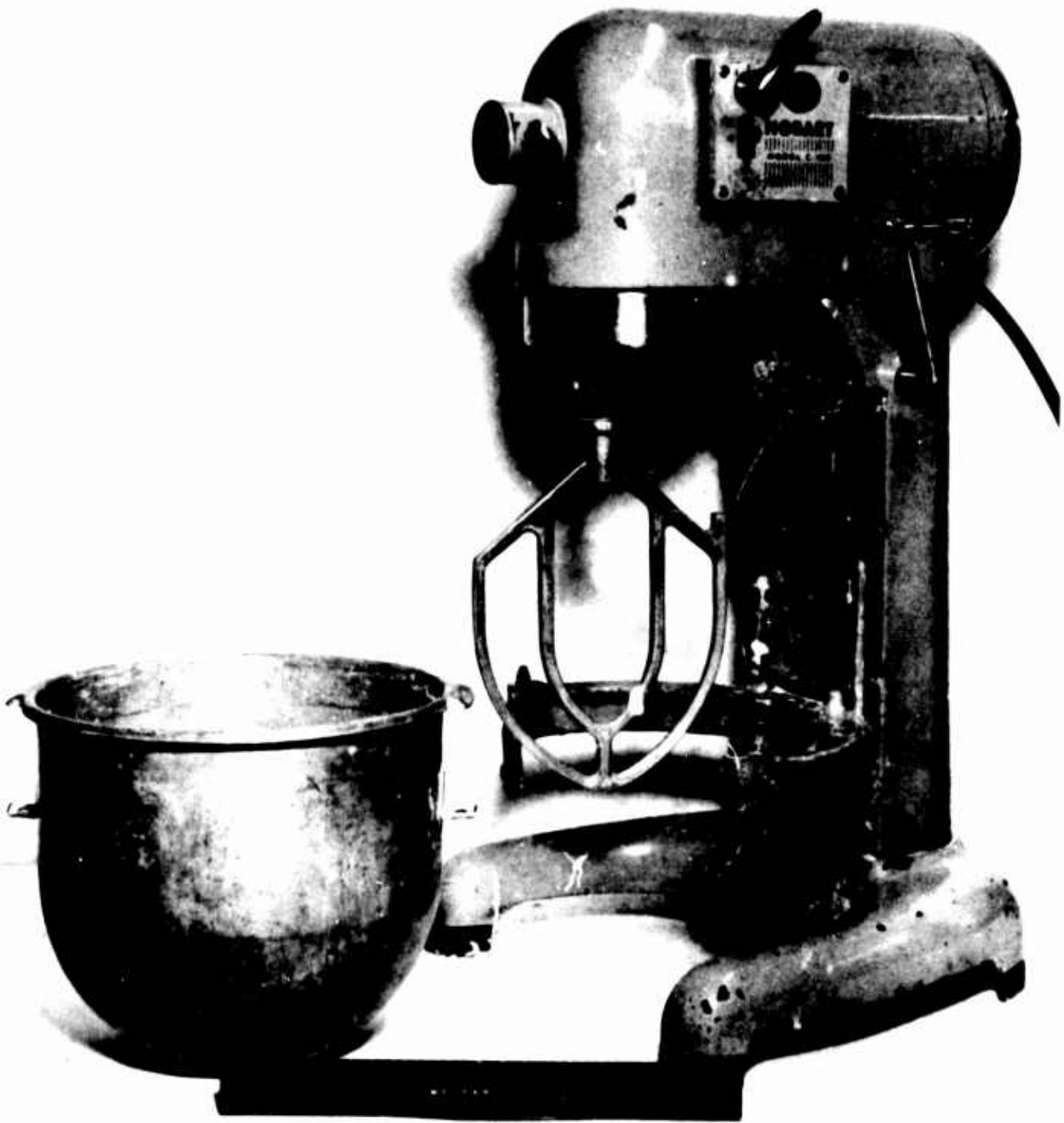


Figure 4. Equipment for Mixing Portland Cement Mortars

early strength portland cement. All specimens in the other series were made from a single bag of ordinary portland cement.

(b) Aggregate: The aggregate used was Ottawa sand conforming to ASTM designation C109.¹⁵

(c) Water: Mixing water was ordinary tap water.

(5) Batch Size

Each batch was made up of the following quantities of materials:

Portland Cement -- 2936 g.

Sand -- 7376 g.

Water -- 1735 g.

(6) Mixing

Mixing was done as specified in ASTM designation C305, part 6.¹⁴

(7) Placing in Molds

Molds were placed in a vertical position. Mortar was added to the mold in lifts of about 1 inch. Each lift was tamped three times with the 50 inch long aluminum tamping rod.

(8) Curing

After molds were filled, they were placed in a tank and kept covered by water. Specimens made with high early strength cement were cured under water for 7 days, air-dried on a rack for 14 days, and tested 21 days after casting. Specimens made with ordinary portland cement were cured under water for 14 days, air dried on a rack for 14 days, and tested 28 days after casting.

In most cases, molds were left on specimens until the under-water cure was completed. In all cases, molds were removed before the start of the air drying period.

d. Method for Determining Static Tensile Strength and Density

(1) Scope

This method covers the procedure for determining static tensile strength of 2-inch-long specimens cut from plaster and cement mortar bars by the cylinder splitting test and determining density.

(2) Apparatus

(a) Testing Machine: The testing machine used was a Tinius Olsen Super "L" with full-scale ranges of 1200, 12,000, and 60,000 lb.

(b) Bearing Block: A Tinius Olsen spherical bearing block with a bearing face diameter of 2.5 inches was positioned between the lower surface of the test specimen and the bed of the testing machine.

(c) Bearing Strips: Two bearing strips of thick blotting paper, approximately 1/2 inch wide, 2-1/4 inches long, and 0.022 inch thick were cut for each specimen. Bearing strips were placed between the specimen and both the upper and lower bearing block of the testing machine. Bearing strips were not reused.

(d) Scales: Specimens were weighed in an Ohaus triple-beam balance, model CG 311, with a least-scale division of 0.01 g.

(3) Test Specimens

Test specimens were 2.0-inch-long segments cut from long bars cast for dynamic test specimens. Cutting was done with the Felker DiMet Model 11-B saw equipped with a diamond blade, shown in figure 5. Diameter of plaster specimens was about 0.95 inch. Diameter of mortar specimens was about 1.2 inches.

(4) Procedure

(a) Measurements: Diameter of the specimen was measured to 0.001 inch along the diameter which contacted the heads of the testing machine. Length of the specimen was measured to the nearest 0.001 inch; the weight of specimens was measured to the nearest 0.01 g, and the breaking load was recorded to the nearest 10 pounds.

(b) Rate of Loading: Load was applied continuously and without shock at a rate of about 500 psi per minute.

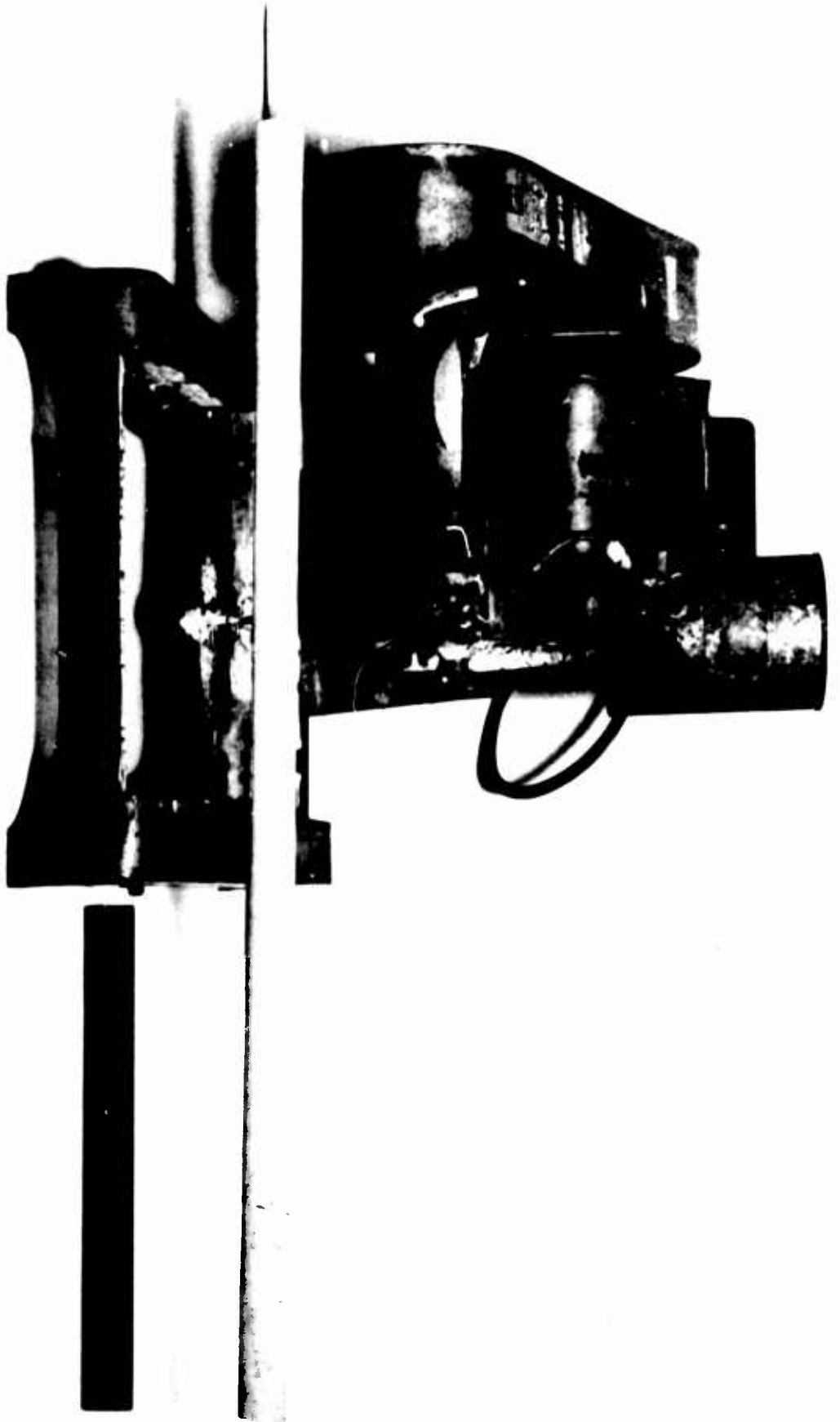


Figure 5. Equipment for Cutting Test Specimens

(c) Density: Density was calculated from the length, diameter, and weight of specimens taken before testing.

(d) Tensile Strength: Splitting tensile strength was calculated as follows:

$$S = \frac{2 P}{\pi L D}$$

where

S = splitting tensile strength in psi

P = maximum applied load indicated by the testing machines in pounds

L = length in inches

D = diameter in inches

(e) Age at Test: Mortar static specimens were tested on the same day as corresponding dynamic specimens.

Ultracal 60 static test specimens were tested after air drying for 13 to 19 days.

Hydrostone static test specimens were tested after air drying for 41 to 55 days with three exceptions at 15, 16, and 24 days.

e. Method for Cutting Test Specimens and Applying Gages and Conductive Strips

(1) Scope

This method covers cutting of plaster and mortar bars, finishing of ends, application of conductive strips, and application of strain gages.

(2) Apparatus

(a) Cutting Machine: Bars were cut with a Felker DiMet Model 11-B saw, shown in figure 6. This saw was equipped with a diamond blade. No lubrication was required for cutting plaster bars. The blade was lubricated with water for cutting cement mortar bars.

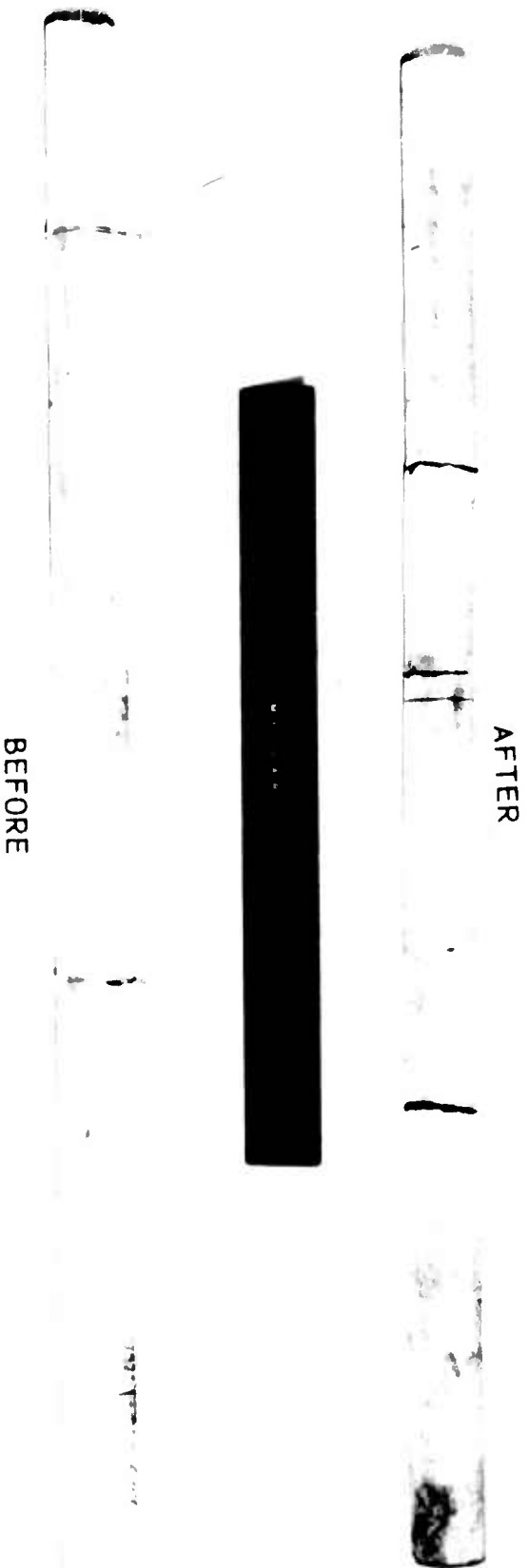


Figure 6. Mortar Dynamic Test Specimens Before and After Testing

(b) Finishing of Ends: A standard machinists V-block and file were used for finishing the ends of plaster bars.

(3) Materials

(a) Conductive Strips: Conductive strips were painted on bars with silver print No. 21-2 printed circuit paint, made by G. C. Electronics Company.

(b) Glue: Strain gages were applied with Duco cement made by duPont.

(c) Strain Gages: Strain gages used were SR-4, types C-8 and A-14, made by Baldwin Lima Hamilton Corp. Gages, type A-14, were used on all specimens made of Hydrostone and high early strength cement, and for most specimens made of ordinary portland cement. Gages, type C-8, were used on all specimens made of Ultracal 60 plaster and a few specimens made of ordinary portland cement.

(4) Location of Gages and Conductive Strips

Location of strain gages and conductive strips is given in table I.

(5) Procedure

Specimens were not handled for cutting until they had air dried for at least 4 days. Care was taken to avoid impacts that might cause internal cracks in the specimens. In many cases, a long bar was cut in half to make two shorter specimens for dynamic tests.

Specimens for determining static tensile strength were 2-inch-long sections cut from the long bars used in dynamic tests. Static specimens were cut from both upper and lower ends of long bars and marked to indicate location from which taken. Two static specimens were taken from the upper ends of bars and two from lower ends of bars for each batch of Ultracal 60. One static specimen was taken from the upper end and one from the lower end in most batches of Hydrostone. In no case was the difference between strength of specimens from the upper and lower ends of bars significant.

Static test specimens were cut from plaster bars before dynamic tests were made on the long bars. Static test specimens were cut from long bars after the long bars had been broken in dynamic tests. Mortar static test specimens were cut from the end of the bar which had been placed against the loading machine anvil. These results were compared to several static

TABLE I

LOCATION OF STRAIN GAGES AND CONDUCTIVE STRIPS

Material	Series	Nominal Specimen Length	Loading Pulse Duration t_2	Distance Free End to Start Conductive Strip	Distance Free End to End Conductive Strip	Distance Free End to Strain Gage d_1	Distance Free End to First Tension d_3
Ultracal 60	1	19	100	3	8	9	5.7
		30	250	8	19	20	14.3
		55	500	16	35	36	27.6
Ultracal 60	2	19	105	3	8	6	5.9
		30	262	8	19	14.5	14.8
Hydrostone	3	19	105	2	11	6.5	6.5
		36	262	5	21	16	16.2
		58	524	10	36	30	32.4
High Early Strength Mortar	4	24	105	3	14	10	8.8
		48	262	6	30	24	20.7
Ordinary	5	24	105	3	14	10	8.1
		48	262	6	30	24	20.1

test samples which had not been fractured dynamically, and the average stress as well as the scatter were approximately equal for each type.

Conductive strips consisted of four thin strips of paint spaced at 90 degrees around the specimen. Thin layers of printed circuit silver paint were terminated in tinned bare copper wires wrapped tightly around the specimens. The surface of the specimens was sanded to remove fiber, etc., before applying silver paint.

Locations at which strain gages were to be applied were sanded to remove surface irregularities and were cleaned with acetone. A coat of Duco cement was applied to the surface and allowed to dry. A second coat of Duco cement was applied, and the gage was pushed down so as to leave no voids in the glue line. A layer of waxed paper was placed over the gage and was followed by a rubber pad. Pressure was applied by rubber bands stretched around the bar. The gage factor was written on the specimen near the gage. Gage factor is the dimensionless relationship between the change of length and change of resistance of an electrical strain gage and is expressed mathematically as

$$F = \frac{\Delta R/R}{\Delta L/L}$$

Cement and silver paint were dried for at least 24 hours before testing. Portland cement mortar dynamic specimens before and after testing are shown in figure 6.

After cutting specimens to length, applying gages, and applying conductive strips, the ends of plaster bars which were to fit against the anvil were filed flat and square using a machinists V-block as a guide. Flatness of ends was checked by pressing the end of the bar against the flat surface of the V-block.

Due to the hardness of concrete, the ends of the concrete bars were not finished further after being cut square with the diamond saw blade.

f. Method for Determining Moisture Content at Time of Dynamic Test

(1) Scope

This method covers determination of percent moisture content, by weight, of dynamic test specimens at time of testing.

(2) Apparatus

The scale used was an Ohaus triple-beam balance, Model CG 311, with a least-division of 0.01 g.

Specimens were dried in a thermostatically controlled oven.

(3) Procedure

Immediately after dynamic testing, a fragment of suitable size (25 g to 300 g) was weighed and marked with its weight to the nearest 0.01 g. Specimens were placed in an oven at 200°F and weighed each day until the weight change in 24 hours was negligible. In all cases, weight change was negligible after 7 days.

Percent moisture at test was computed as

$$\frac{100 (\text{weight at dynamic test} - \text{weight after baking})}{\text{Weight at dynamic test}}$$

g. Method for Dynamic Fracture Testing

(1) Scope

This method covers the loading apparatus, measuring equipment, and procedure for dynamic fracture tests of plaster and portland cement mortar bars.

(2) Loading Apparatus

A special purpose loading apparatus was constructed by Melpar specifically for this experimental investigation.

The loading apparatus is shown schematically in figure 7. Note that the loading apparatus passes through a wall, so that the specimen holder is in a dark room, but the rest of the apparatus is in a lighted laboratory.

Details of the metal bars are shown in figure 8. An end view of the loading apparatus is shown in figure 9.

Figure 10 is a photograph of the loading apparatus and measuring equipment in the lighted laboratory. Figure 11 is a photograph of the dark-room showing a specimen in the specimen-holding fixture ready for test.

In essence the loading device provides: (1) a fixture of very low acoustic impedance for holding a specimen in intimate contact and accurate alignment with the anvil bar, (2) supports of low acoustic impedance and low coefficient of friction for the anvil and striker bars, (3) a rigid and accurate guide to maintain alignment of the anvil and striker bars, and (4) a latching

mechanism and a compressed air propulsion system for the striker. The loading apparatus operated very well at plenum pressures between 5 and 30 psi, with stress in the steel bars varying from 1500 psi to 21,000 psi. Control was better at high pressures than at low pressures. For operation below 5-psi plenum pressure (necessary in tests of concrete mortars), the O-ring was removed. Below 5 psi, friction in the barrel due to dust, etc., was significant, and control of velocity became difficult.

The entire guidance and support apparatus was made quite heavy. The barrel which controls alignment of the striker and anvil bars has an inside diameter of 2.00 inches and a wall thickness of 1/4 inch. The bed of the apparatus is a 20 ft long, 12-inch by 3-inch steel channel, weighing 20.7 lb per ft, or a total of 414 lb. Teflon rings supporting the anvil and striker bars were fitted to the bars and tube so that no lateral movement could be detected, but bars would slide smoothly and freely in the barrel.

The angle-iron framework, visible in figure 12, was made to slide along the bed of the loading apparatus and could be raised or lowered to adjust the field of view of the camera. In addition to supporting the camera, this framework supported the outer end of some test specimens. All concrete specimens of 48-inch nominal length and all plaster specimens of 50- to 6-inch lengths were partially supported by a cord extending from the outer end of the specimen vertically to the top horizontal member of the angle-iron frame.

(3) First Instrumentation Setup

(a) Electronic Equipment: A block diagram of instrumentation used in the first series of tests is shown in figure 12. This setup was used for the first series of tests, Ultracal 60 Series 1, but was not used further because it was found that the break of the silver conductive strip on the specimen was not a sufficiently accurate measure of time of completing fracture of the specimen.

When the striker bar contacted the anvil bar, a trigger pulse was delivered to the Tektronix 535 Oscilloscope, starting its sweep, and causing generation of a delayed trigger pulse to the Tektronix 502 Oscilloscope.

When the conductive strip on the specimen was broken, a pulse was delivered to one channel of the 502 Oscilloscope and also to the first Dumont 404 pulse generator. This generator delivered a trigger pulse to the remaining pulse generators after a delay of a few microseconds, and triggered the first strobe light after a delay of up to 100 microseconds. The Teletronics pulse generator fired the second strobe light after a delay of up to 1 millisecond.

BLANK PAGE

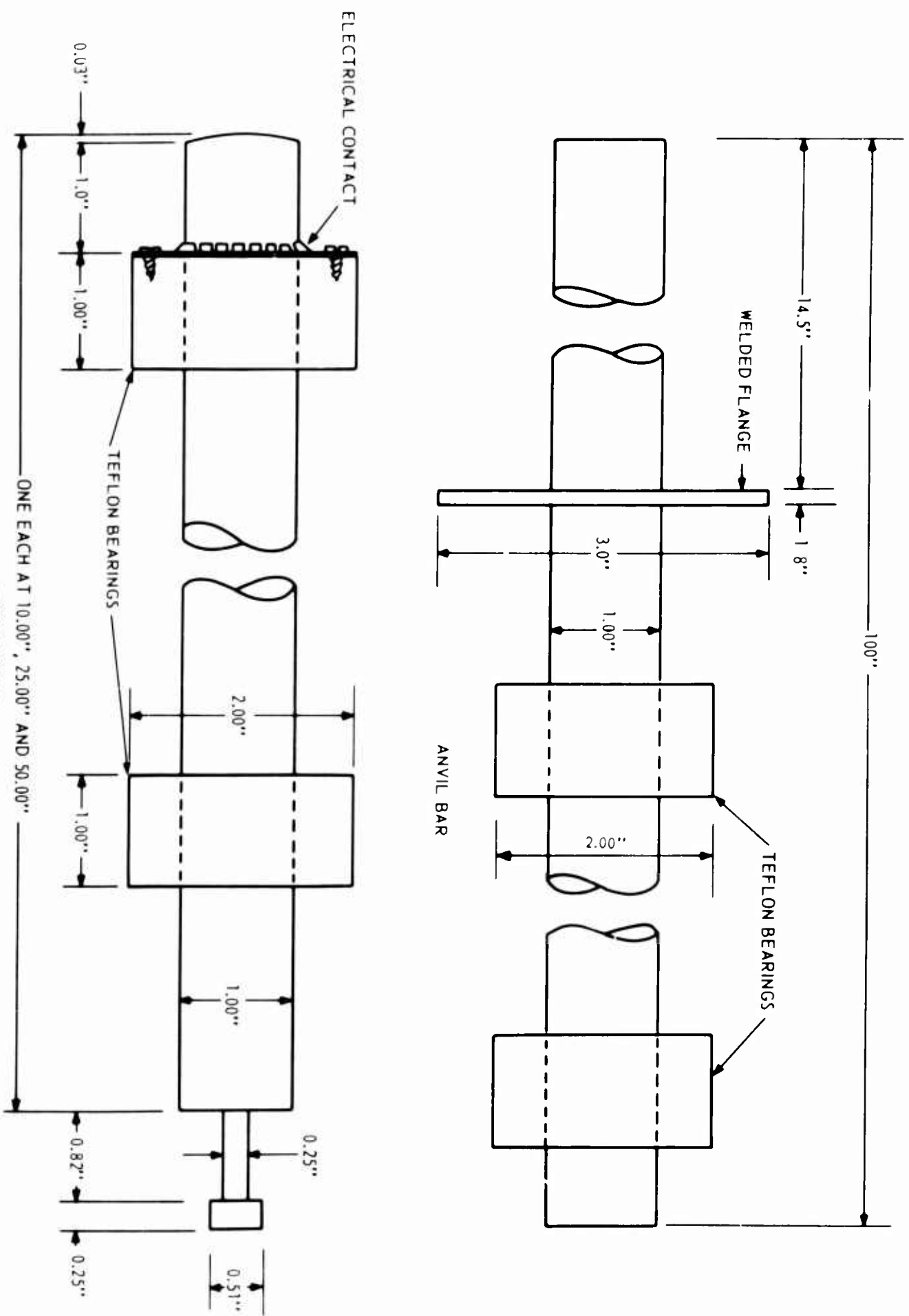


Figure 8. Details of Anvil and Striker Bars

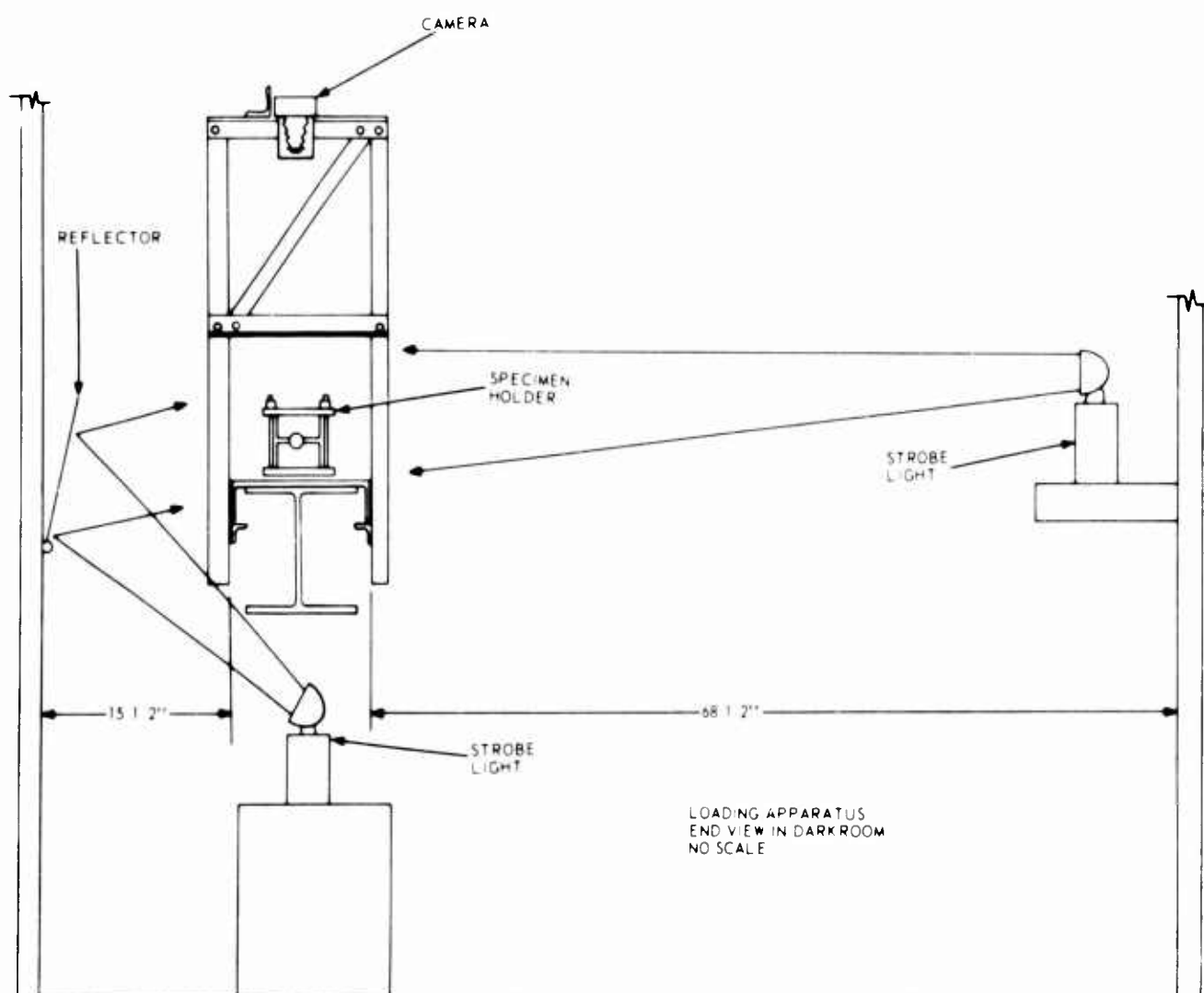


Figure 9. End View of Loading Apparatus

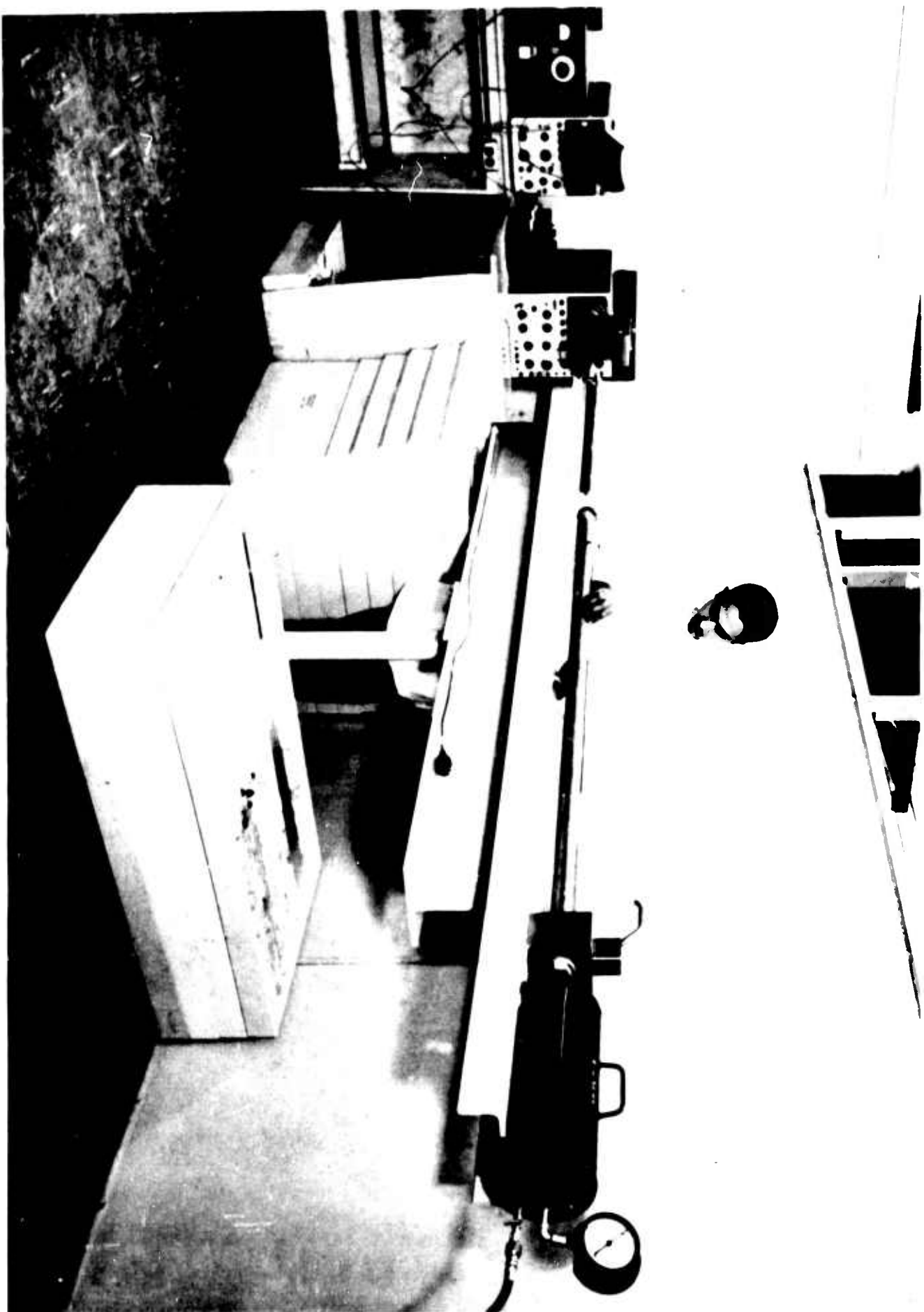
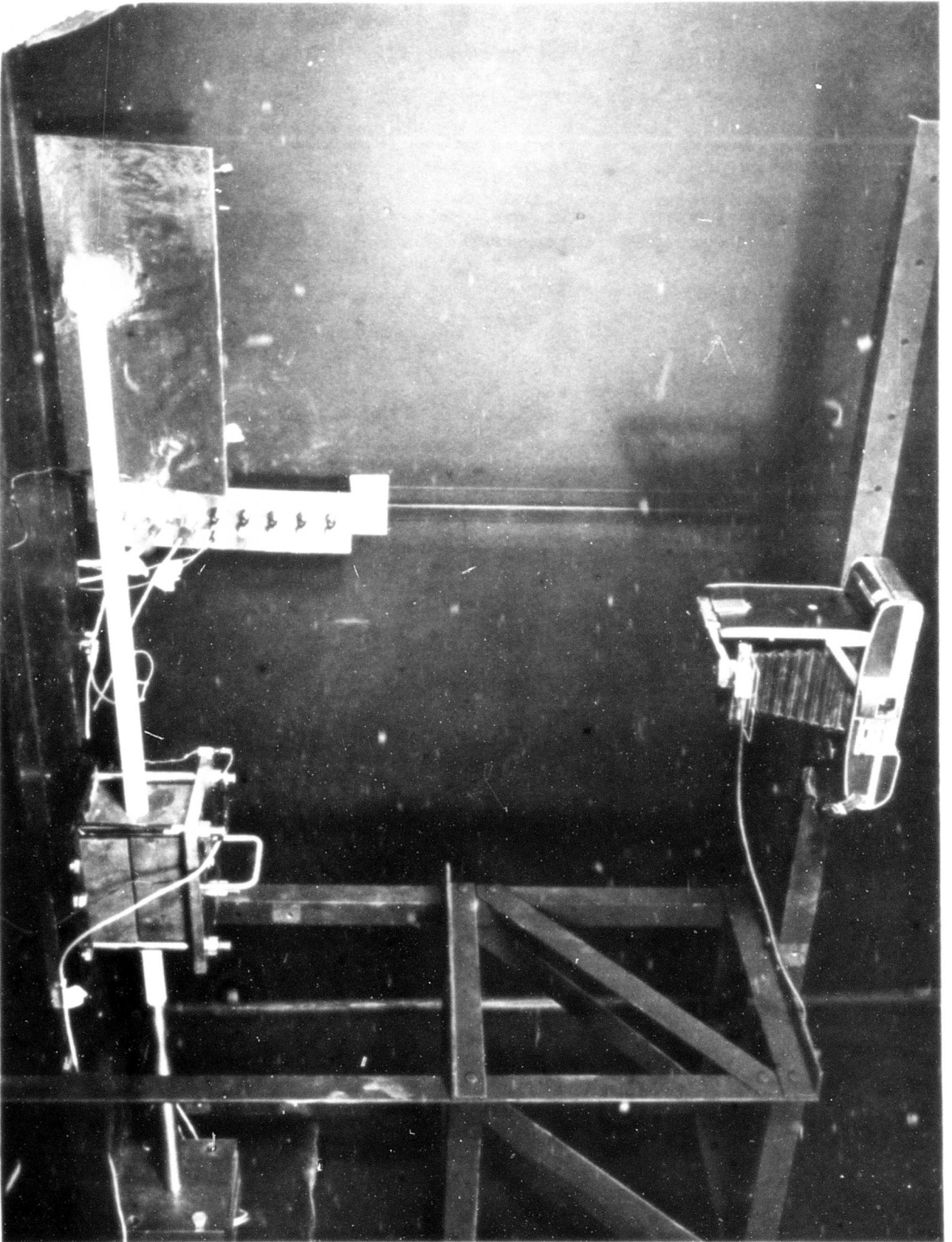


Figure 10. Photograph of Loading Apparatus Outside Darkroom

Figure 11. Photograph of Loading Apparatus Inside Darkroom



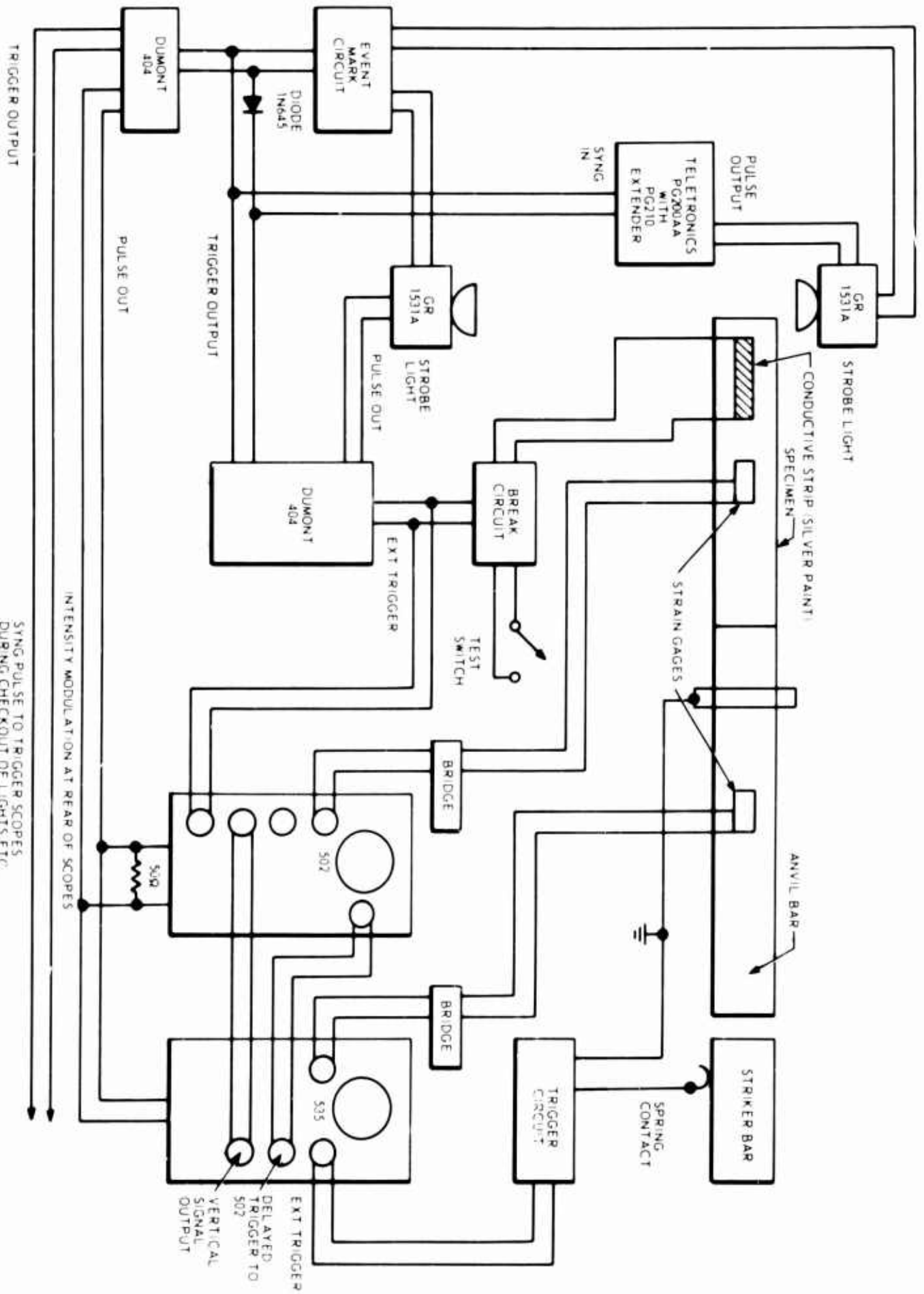


Figure 12. First Test Equipment Block Diagram

When the first Dumont 404 pulse generator or either strobe light fired, the second Dumont 404 pulse generator was triggered and immediately generated a pulse which produced an intensity-modulated event mark on both oscilloscopes.

The camera in the darkroom (see figure 11) recorded an image of the specimen when each strobe light was fired. Each light illuminated only one side of the specimen. The first light was timed to produce a picture as soon as the first fracture had opened enough to be visible. The second light was timed to produce a picture as soon as all fractures were opened enough to be visible. Intensity-modulated event marks on records from the two oscilloscopes showed the exact time at which pictures were taken.

The single-channel 535 oscilloscope recorded strains in the anvil bar, time of break of conductive strip, and time of firing of each strobe light. The 502 oscilloscope recorded strains in the specimen, time of break of the conductive strip, and time of firing of the first strobe light. Sweep time on the 502 was usually too short to record firing of the second strobe light.

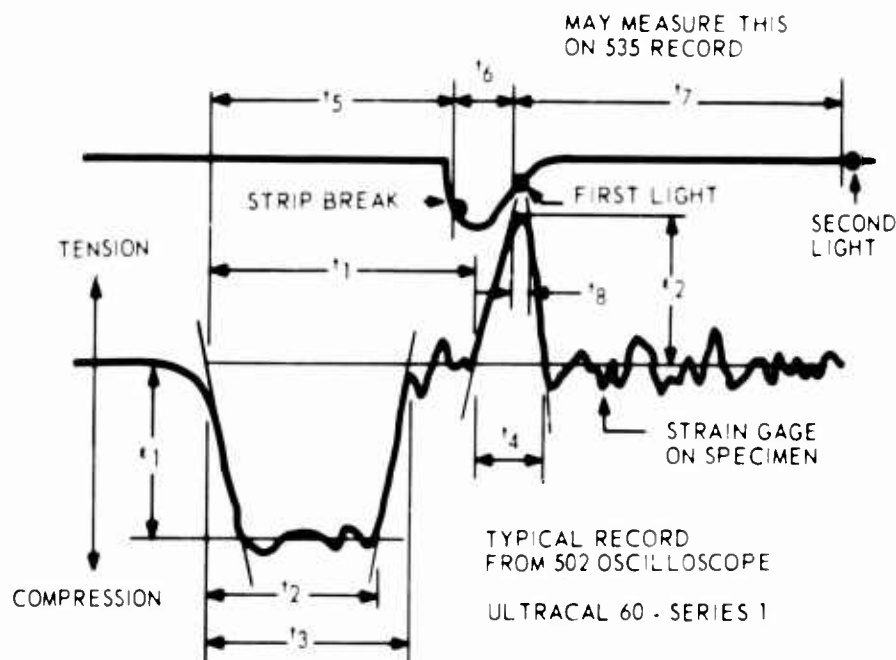
(b) Measurement: Original data consisted of a photograph showing two stages in the fracture of the specimen, a photograph of the screen of the 502 oscilloscope showing strain history at a gage on the specimen, the time of break of the conductive strip, the time of firing of the first strobe light, a photograph of the screen of the 535 oscilloscope showing strain history in the anvil bar, the time of break of the conductive strip, and the time of firing of both strobe lights.

A sketch of a typical record from the 502 oscilloscope is shown in figure 13. Lines were scribed on the original photograph through the center of the traces, and measurements were taken between the scribed lines. Values could be estimated to the nearest 0.02 cm.

Values of momentum in fragments outboard of the first fracture were computed from the photograph of two stages in the fracture of the specimen and from known times of taking photographs, as indicated in figure 14. Measurements of crack width on the photograph were made with a zoom microscope having a calibrated graticule and reading directly to 0.001 inch.

(4) Second Instrumentation Setup

(a) Electronic equipment: A block diagram of instrumentation, used in all testing except the first series, Ultracal 60, series 1, is shown in figure 15. Circuit diagrams for the trigger circuit, the event mark circuit, and the break circuit and bridge circuits are shown in figure 16. A photograph of the recording equipment is shown in figure 17.



- ϵ_1 = COMPRESSIVE STRAIN MAGNITUDE
 ϵ_2 = TENSILE STRAIN MAGNITUDE
 $T = \frac{t_1 + t_3}{2}$ = INTERVAL BETWEEN ARRIVAL OF
 COMPRESSION PULSE AND FIRST
 TENSION

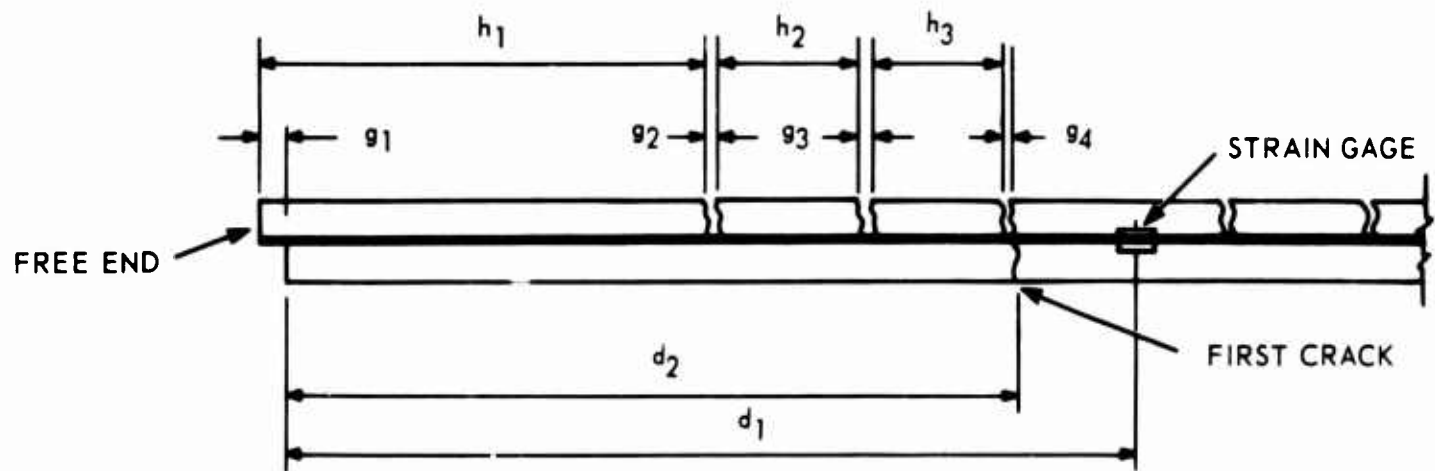
Figure 13. Sketch of Data from First Series of Tests with Notation

This instrumentation setup differs from the first setup in that the time of breaking the conductive strips and firing of the strobe lights was not recorded. Time between firing of the strobe lights was calibrated, but was not recorded for each shot.

When the striker bar contacted the anvil bar, a trigger pulse was generated which started the sweep on the 502 oscilloscopes after an appropriate delay. This oscilloscope subsequently recorded strains measured by gages on the anvil and specimen.

When the conductive strip was broken, a pulse was generated which, after appropriate delays, caused pulse generators to trigger the strobe lights. The 535 oscilloscope was used to record time between the firing of the two strobe lights.

The camera in the darkroom (see figure 11) recorded an image of the specimen when each light fired. Each light illuminated only one side of the specimen, so that an image of first one side and later the other side was recorded on the film. The first light was timed to produce a picture as soon



$$M_1 = \rho d_3 C \epsilon_1 = \rho t_2 C^2 \epsilon_1$$

= TOTAL PARTICLE MOMENTUM/UNIT AREA IN INCIDENT COMPRESSIVE PULSE

$$M_2 = \rho C \epsilon_1 \left[d_3 + d_2 \cdot C (t_5 - T) \right]$$

= PARTICLE MOMENTUM/UNIT AREA IN FRAGMENTS BETWEEN FIRST CRACK AND FREE END (USING BREAK STRIP DATA)

$$M_3 = \frac{\rho}{t_7} \left[h_1 g_1 + h_2 (g_1 - g_2) + h_3 (g_1 - g_2 - g_3) + \dots \right]$$

= PARTICLE MOMENTUM/UNIT AREA IN FRAGMENTS BETWEEN FIRST CRACK AND FREE END (USING PHOTOGRAPH DATA)

$$M_4 = \rho C^2 \epsilon_2 \left[\frac{t_4 + t_8}{2} \right]$$

= PARTICLE MOMENTUM/UNIT AREA IN REFLECTED PULSE PASSING STRAIN GAGE

Figure 14. Sketch of Measurements on Photograph of Specimen with Notation

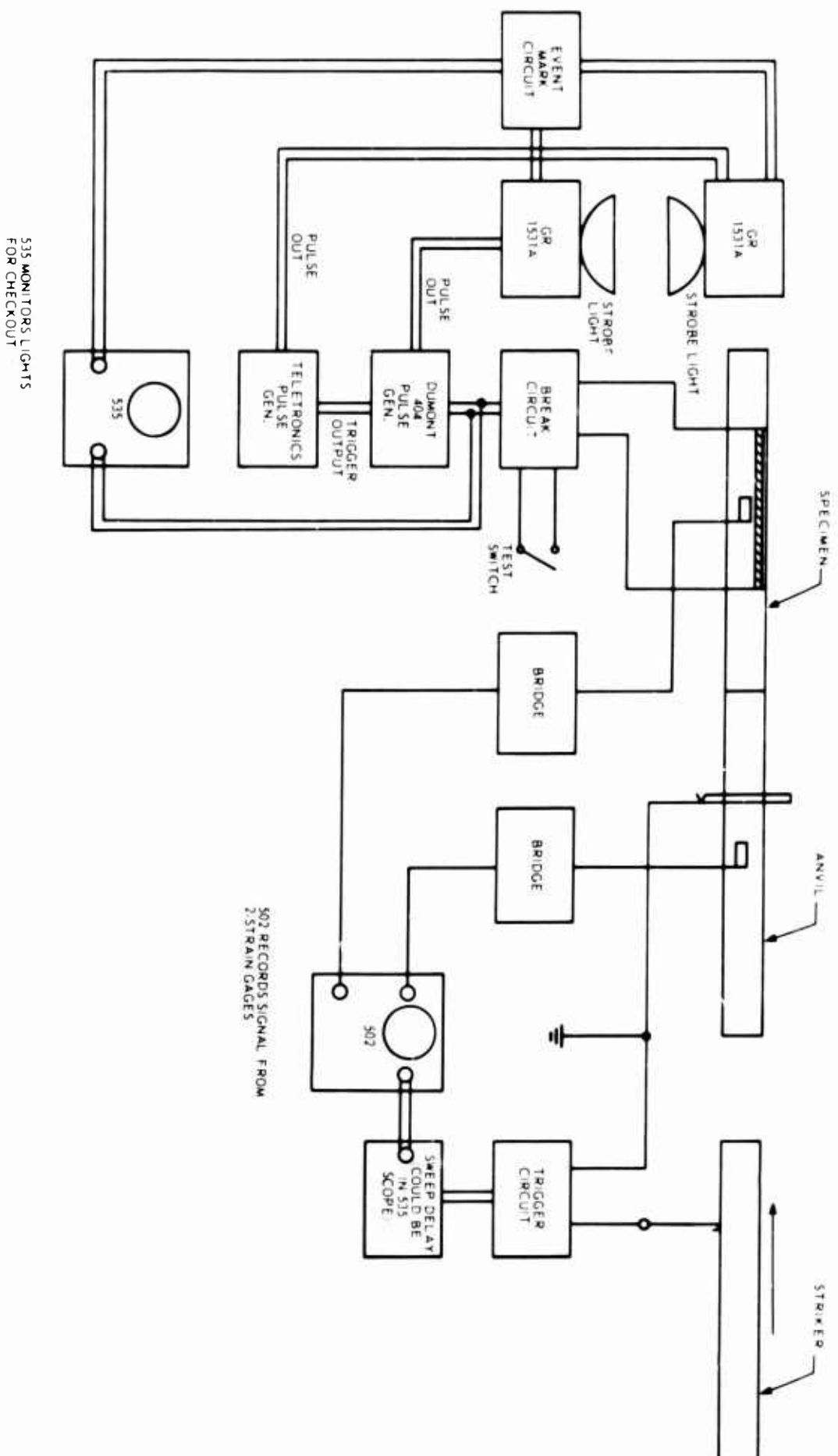
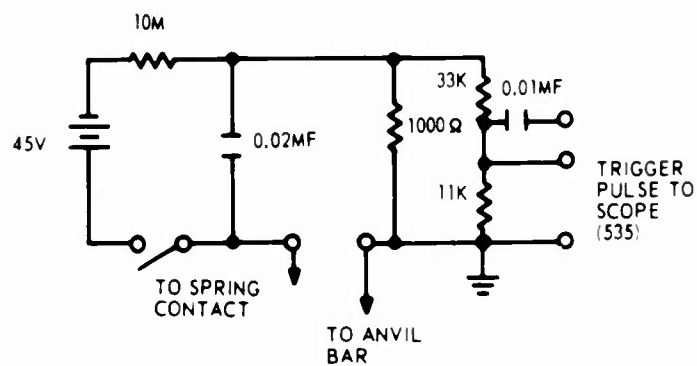
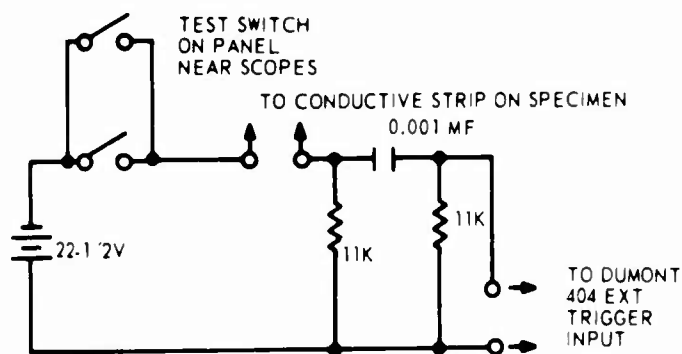


Figure 15. Second Test Equipment Block Diagram

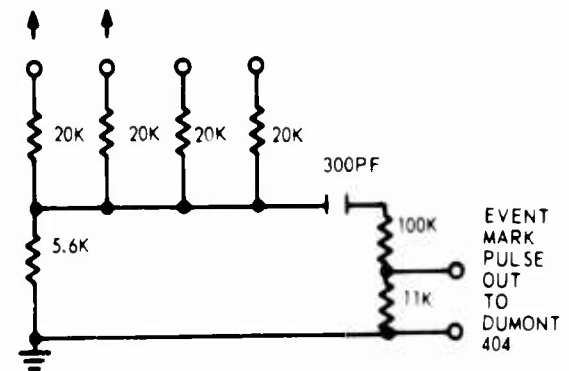


TRIGGER CIRCUIT

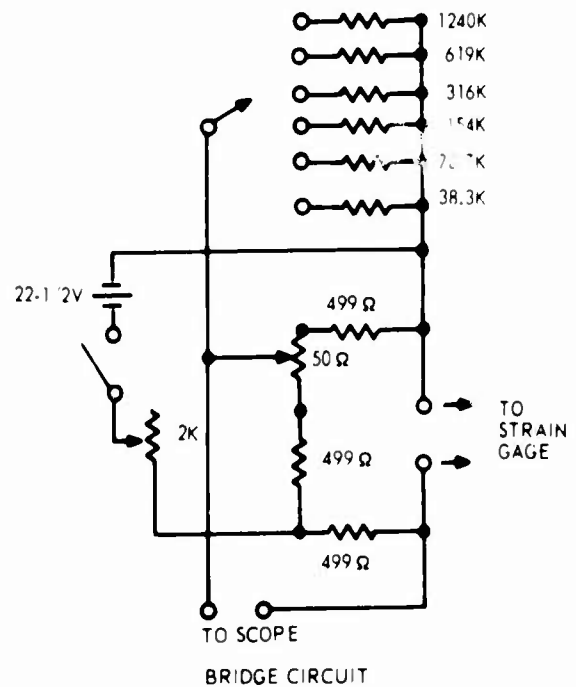


BREAK CIRCUIT

TO 1531A STROBE LIGHTS



EVENT MARK CIRCUIT



BRIDGE CIRCUIT

Figure 16. Circuit Diagrams

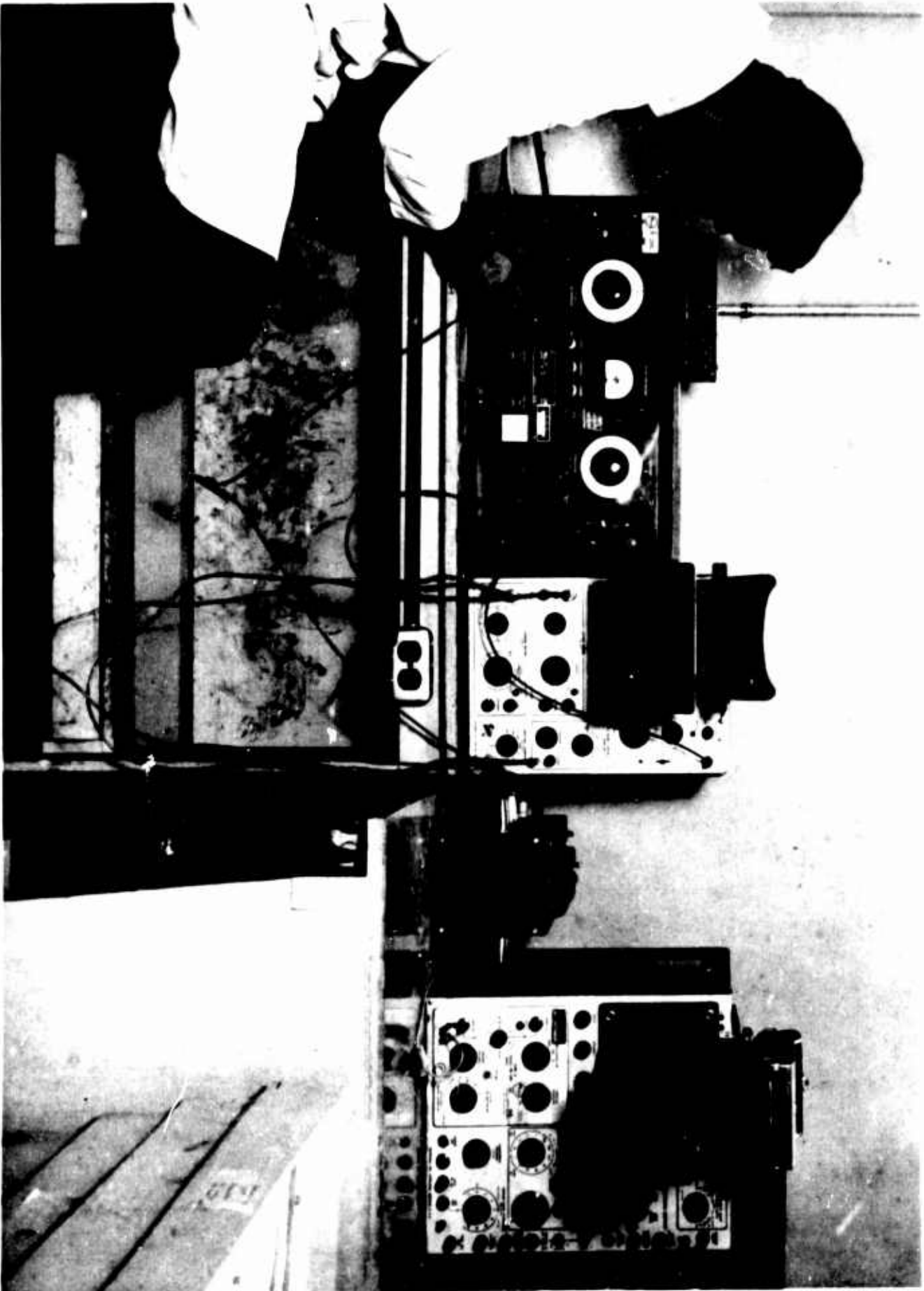


Figure 17. Photograph of Recording Equipment

as the first fracture had opened enough to be visible. The second light was timed to produce a picture as soon as all fractures were opened enough to be visible.

(b) Measurement: Original data consisted of a photograph showing two stages in the fracture of the specimen and a photograph of the screen of the 502 oscilloscope showing records of strain on the anvil and specimen.

A sketch of a typical record from the 502 oscilloscope is shown in figure 18. Lines were scribed through centers of traces on the original photographs, and measurements were taken between the scribed lines. Photographs of original data are shown in figure 19.

(5) Test Specimens

Dynamic test specimens were slender bars having diameters between 0.9 and 1.2 inches and lengths between 18 and 60 inches. Figure 6 shows typical portland cement mortar specimens ready for testing and after testing. Figure 11 shows a specimen in place for test.

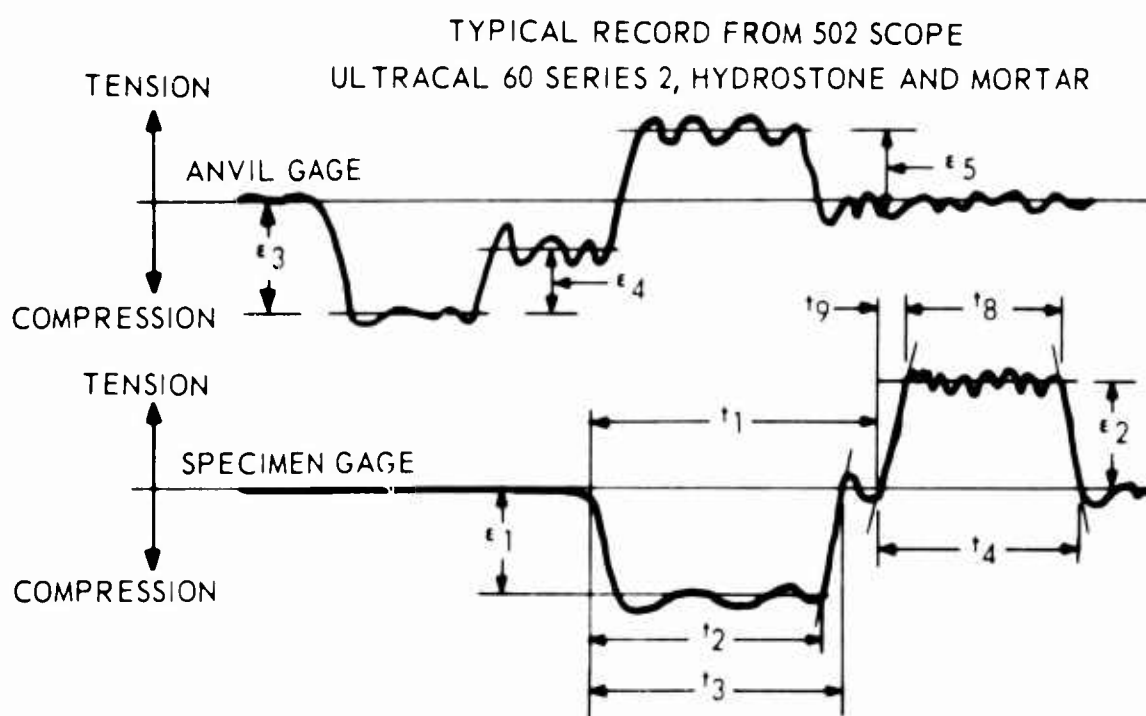
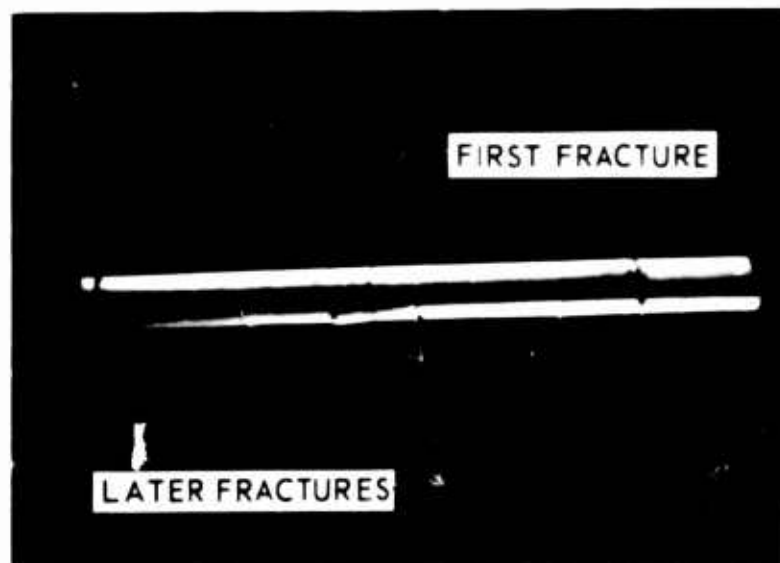
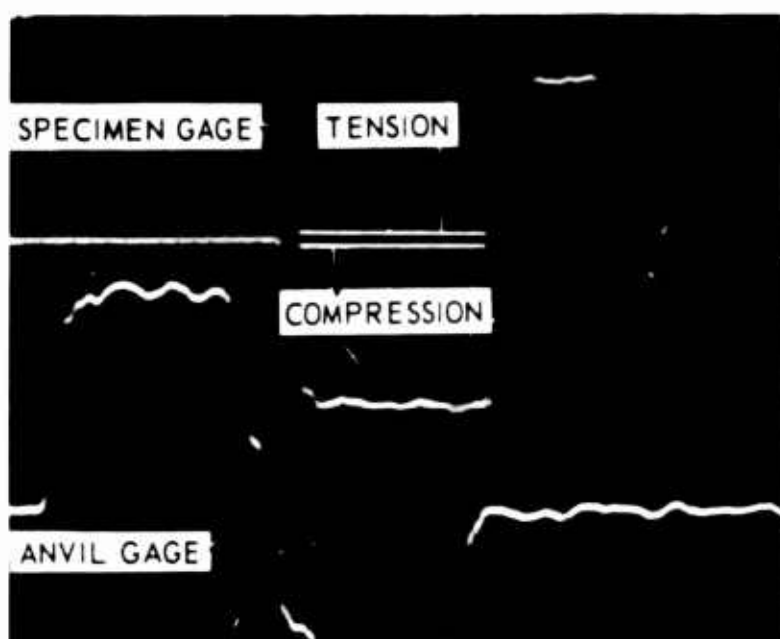


Figure 18. Sketch of Data from Tests Excepting First Series



(a)



(b)

Figure 19. Photograph of Original Data from Tests Excepting First Series

(6) Procedure

Specimens were prepared as described in Method for Cutting Test Specimens and Applying Gages and Conductive Strips.

The specimen was placed in the holding fixture and aligned so that its end fitted squarely against the end of the anvil bar. The holding fixture was then moved back so that there was a clearance of about 1/4 inch between the anvil bar and the specimen. All wire connections were then made to the strain gage and the conductive strip. Care was taken to insure that wires would neither impede the motion of fragments of the bar during fracture nor cast undesirable shadows in photographs.

Checkout of loading and measuring equipment was done according to a detailed two-page checklist. Checkout included the operation of the loading machine, the triggering circuitry, strobe lights, calibration checking of the strain-gage circuitry, film checking in the cameras, and the setting of controls on oscilloscopes and cameras. A data sheet was filled out which included a dimensional sketch of the specimen, the specimen number, the gage factor, the calibration data, and the setting of all controls.

Grease was applied to the end of the anvil bar, and the specimen-holding fixture was moved so as to bring the specimen squarely against the end of the anvil bar and press out most of the grease so as to leave the thinnest possible layer.

The test was carried out, again following a check list to insure that each component of equipment was properly set. After the specimen was broken, the pieces were recovered and reassembled in a tray. Trays of broken specimens are visible in figure 10. A piece of the specimen was weighed for later determination of percent moisture at test. Photographs from the oscilloscope camera and the specimen camera were labeled and attached to the data sheet having calibration data and so forth.

Lines were scribed on the photographs and initial measurements taken soon after the specimen was tested.

SECTION 4

RESULTS

A summary of material properties is contained in table II, and tabulated data for each of 321 dynamic tests are contained in tables III to VII. These tabulated data make it possible to reconstruct a good approximation of the tensile phase strain history for each dynamic test specimen. Also, a number of calculated quantities are tabulated.

Table II contains mean values and standard deviations for measurements of pulse velocity, density, and static tensile strength; the percent of moisture at test and the parameter, K , defined by Martin and Murphy;¹¹ and average values of some other calculated parameters. It should be recalled that if a variable is normally distributed the mean plus or minus one standard deviation includes 68.3 percent of the population, and the mean plus or minus two standard deviation includes 95.4 percent of the population.

Standard deviation of measurements of pulse velocity, density, and percent moisture at test are small percentages of mean values, or small in absolute value. It appears from these measurements that test specimens had a good degree of uniformity. Standard deviation in static tensile strength measurements ranged from 18.5 to 22.9 percent of the mean values. This is higher than is usually found in concrete testing; but concrete test specimens customarily have a high moisture content, whereas all specimens in this investigation had quite low moisture contents. Scatter of this magnitude is not unusual in impact tests of metals below their transition temperature.

It will be seen in figures 20 through 23 that scatter of data in dynamic tests was little greater than in static tests.

Some idea of the degree of scatter anticipated by the writers of the standard "Test for Tensile Strength of Hydraulic Cement Mortars," ASTM C 190-63,¹⁶ can be had by examining criteria for faulty briquets and retests. The minimum number of test specimens to be made for a given curing condition is three. The minimum number of test specimens to be used as a valid measure of strength is two. Strength values differing from the mean by more than 15 percent are to be discarded.

Testing technique would still be considered acceptable if as many as one-third of the test specimens deviated from the mean by more than 15 percent. This implies a standard deviation slightly above 15 percent of the mean. Also, ASTM C-190-63 specifies testing specimens saturated with moisture, which probably results in less scatter than if they were dry.

No data was taken to determine the deviation of materials tested in this investigation, if any, from Hooke's law for loading up to fracture in tension. It is thought that this deviation is negligible. It should be noted that strain was measured directly in dynamic tests, Young's Modulus was calculated from density and pulse propagation velocity, and static tensile stress was calculated according to ASTM Designation C496-64T¹⁷ from force required to split a cylinder. If there was any deviation from Hooke's law, it is more valid to compare calculated dynamic stress to static stress than to compare measured dynamic strain to calculated static strain.

Dynamic tests employed three striker bars, producing loading pulse duration of about 100, 250, and 500 microseconds. In each series of tests an attempt was made to find the maximum strain at which specimens were not fractured by pulses of each duration. Specimens which did not fracture during the first tensile phase are so designated in tables III to VII and plots of these data in figures 21 through 24.

A strain pulse, once in a bar, continues to travel up and down the bar until its energy is absorbed in the material, transmitted to supports and air, or until fracture occurs. Consequently, some specimens fractured as a result of the first loading pulse but not during the first tensile phase.

Some specimens were not fractured by the first dynamic load applied. In most cases, these specimens were retested at a higher load intensity. When a specimen was loaded dynamically more than one time, the first test is designated in the tables by a specimen number with a suffix, T-1, the second test by the same specimen number with a suffix, T-2, etc.

A few dynamic specimens of ordinary portland cement mortar were broken, glued back together, and broken again. Each broken end which was to be reglued was coated with Eastman 910 primer and air dried for about 5 minutes. One of the two ends which were to make contact was coated with Eastman 910 adhesive. The two ends were pressed together by hand for about 20 seconds to form a bond. After gluing, specimens were allowed to set undisturbed for about 4 hours.

Specimens numbered 97C, 105C, 106C, 107C, 109C and 119C were broken, glued together with Eastman 910 adhesive, and broken again. In only one case did a fracture in the second testing occur in a glue line. Specimens 106C and 107C were instrumented on both the first and second tests. In both cases, the peak strain was higher in the second test than in the first.

It is believed that there is a good chance that natural rock cores, fractured in extraction, can be glued in this fashion to make the long-bar specimens required for this type of dynamic test on natural rocks.

TABLE II
PROPERTIES OF MATERIALS

Material	Pulse Velocity c (in./sec)	Density ρ $\left(\frac{10^{-4} \text{ lb-sec}^2}{\text{in.}^4} \right)$	Static Tensile Strength S (psi.)	Acoustic Impedance pc $\left(\frac{\text{lb-sec}}{\text{in.}^3} \right)$	Modulus of Elasticity E (10^{-6} psi.)	Moisture at test q (weight)	K (10^{-5} sec)	Maximum Pulse Duration for K (10^{-6} sec)	Calculated Strain $\frac{S}{E}$ $\left(\frac{\text{pc}^2}{10^{-6}} \right)$ (in./in.)
Ultracal 60 Series 1	No. of Readings Mean Standard Deviation Std. Dev. % of Mean	14 114,571 3,560 3.12	50 1,485 0.0285 1.92	50 634 124 19.6	- 17.01 - -	- 1,950 - -			325 64
Ultracal 60 Series 2	No. of Readings Mean Standard Deviation Std. Dev. % of Mean	39 112,533 3,950 3.51	40 570 117 20.5	- 16.52 - -	- 1,858 - -	10 18.09 0.23 1.27	19 4.51 0.87 19.3	80	307 63
Hydrostone	No. of Readings Mean Standard Deviation Std. Dev. % of Mean	42 123,428 3,190 2.58	43 980.7 181 18.5	- 19.46 - -	- 2,402 - -	10 18.74 0.20 1.07	59 3.12 1.32 42.3	80	498 75
High Early Strength Portland Cement Mortar	No. of Readings Mean Standard Deviation Std. Dev. % of Mean	47 158,785 8,420 5.3	61 654 128 19.6	- 34.09 - -	- 5,413 - -	16 5.27 0.62 11.8	14 2.87 1.04 36.4	85	121 24
Ordinary Portland Cement Mortar	No. of Readings Mean Standard Deviation Std. Dev. % of Mean	60 153,100 9,360 6.1	62 546 125 22.9	- 32.21 - -	- 4,932 - -	10 4.00 0.37 9.25	14 2.34 1.22 52.3	50	111 25

BLANK PAGE

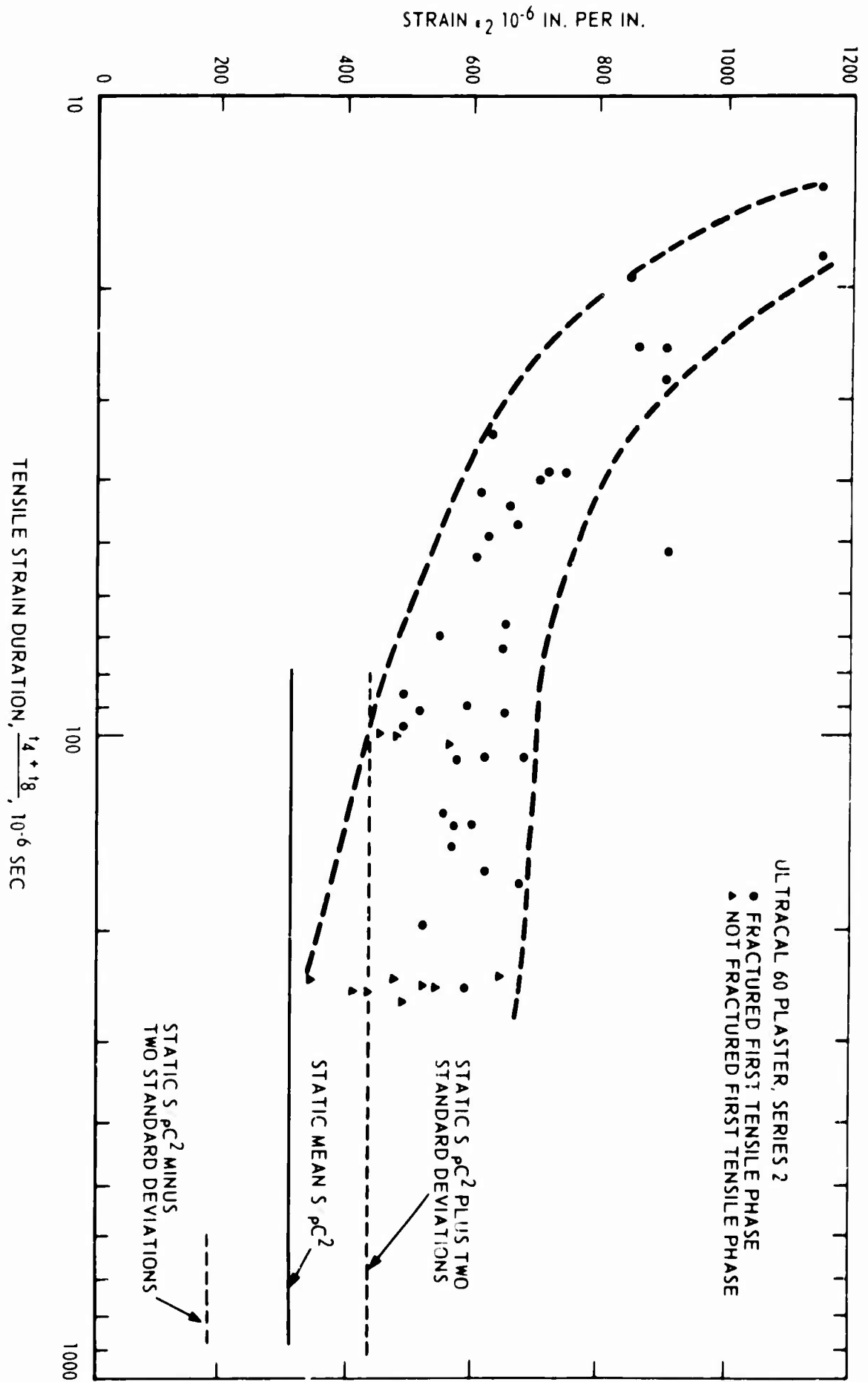


Figure 20. Strain Magnitude vs. Strain Duration for Ultracal 60, Series 2

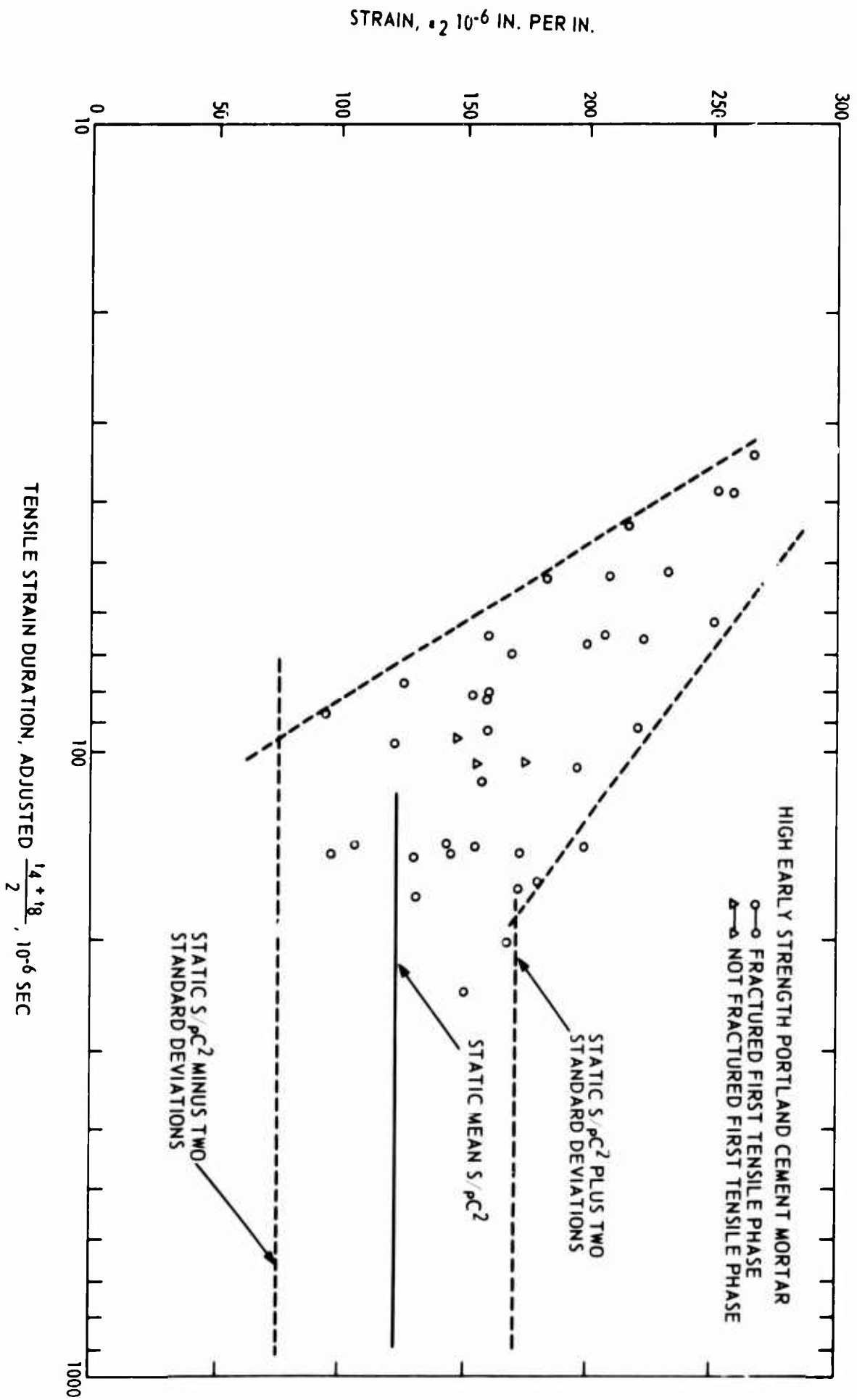


Figure 22. Strain Magnitude vs. Strain Duration for High Early Strength Mortar

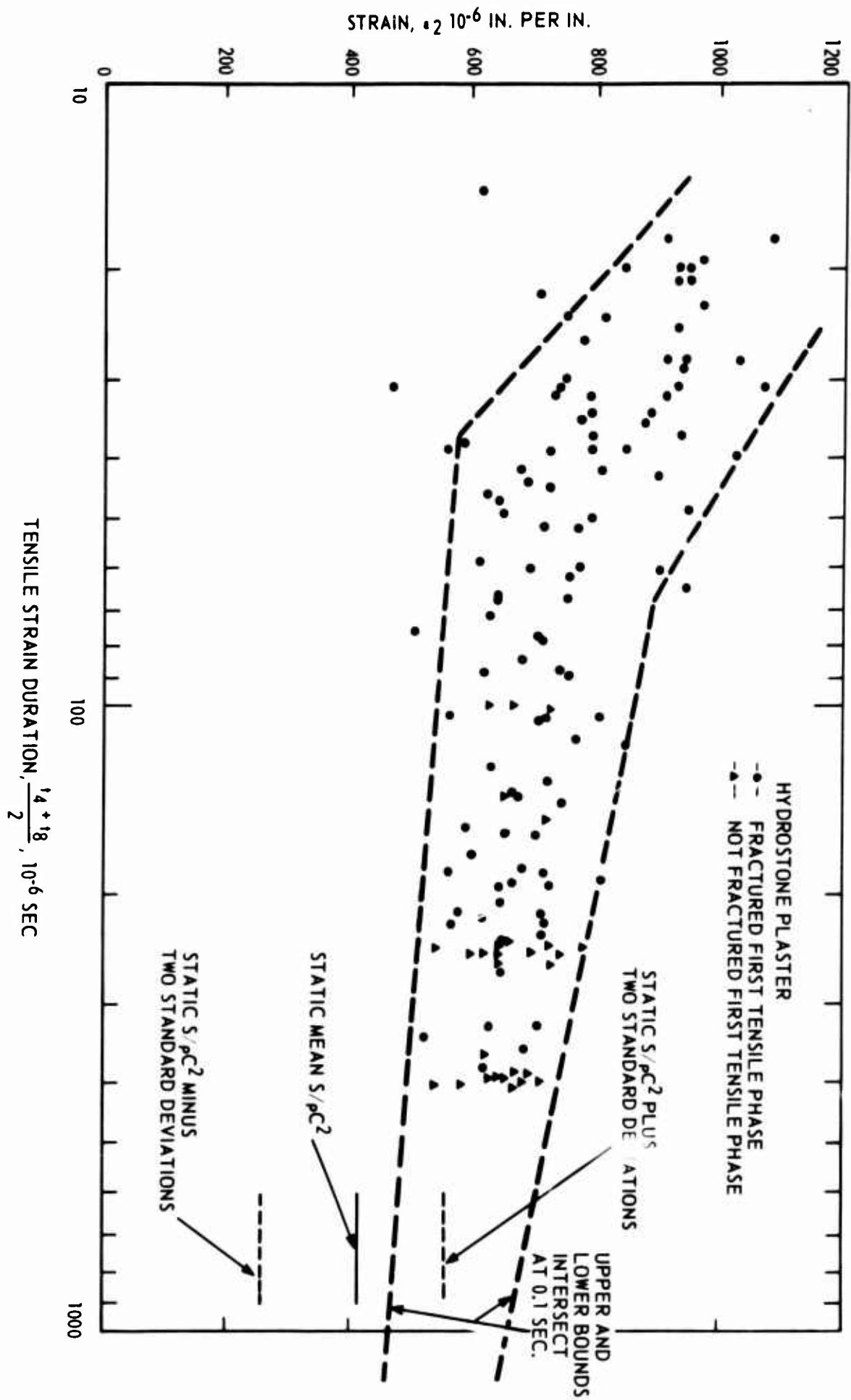


Figure 21. Strain Magnitude vs. Strain Duration for Hydrostone

a. Ultracal 60 Series 1

In this series of experiments, the strain gage was placed further from the free end of the specimen than the section at which the first tension was expected so that the entire compressive pulse could be recorded without interference from the reflected tensile pulse. Location of strain gages, nominal specimen lengths, pulse durations and average distance from the free end to the section first subjected to maximum tension are given in table I. Experiments were planned to test the validity of strain gage measurements, time of photographing the specimen during fracture, and time of fracture indicated by the break of conductive silver strip painted on the specimen.

Momentum of particles in the specimen was calculated from the measurements and equations given in figures 14 and 15, and are presented in table III.

Calculation of the total particle momentum per unit area of specimen in the incident compressive pulse, M_1 , and total particle momentum per unit area of specimen in the reflected tensile pulse reaching the strain gage, M_4 , depended on accuracy of strain gage measurements and time calibration of the oscilloscope.

Calculation of the total particle momentum per unit area of specimen in fragments between the first fracture and free end (using break strip data), M_2 , depended on strain gage measurements, time calibration of the oscilloscope, and time of first fracture indicated by the break of a conductive silver strip painted on the specimen.

Calculation of total particle momentum per unit area of specimen between the free end and first fracture (using photographic data), M_3 , depended on measurements of displacement of fragments on pictures of the specimen taken during fracture and time calibration of the oscilloscope.

It was found that M_2 was always smaller than M_3 , the average ratio of M_2 to M_3 being 0.73, whereas if all measurements were valid M_2 should equal M_3 . It was concluded that time of breaking the conductive silver strip was not a satisfactory measure of time of completing fracture of the specimen. Evidently the silver paint exhibited some ductility and did not fracture until after fracture of the specimen was completed. Time of breaking the silver paint strip was not used as a measure of time of fracturing the specimen in subsequent tests.

The average ratio of $M_1 - M_4$ to M_3 was 1.07, or if one questionable value was omitted, 1.04. This was taken as strong evidence that strain measurements during fracture were valid. The average ratio of $M_1 - M_4$ to M_3

TABLE III
DATA FROM DYNAMIC TESTS OF ULTRACAL 60 SERIES I

Specimen Number	Not Fractured First Tensile Phase	ϵ_1 (10^{-6} in./in.)	ϵ_2 (10^{-6} in./in.)	t_2 (10^{-6} sec)	t_4 (10^{-6} sec)	t_8 (10^{-6} sec)	σ (in./sec)	$\frac{M_1}{P}$ (in./sec)	$\frac{M_2}{P}$ (in./sec)	$\frac{M_3}{P}$ (in./sec)	$\frac{M_4}{P}$ (in./sec)	$\frac{M_1 - M_4}{M_3}$
42		639	606	494	240	186	115,000	4180	2180	2495	1710	0.99
59		551	528	471	228	171	118,000	3620	1421	2210	1470	0.97
53		1900	243	104	9	0	107,000	2260	1610	2068	13	1.09
46		775	723	100	38	0	114,600	1025	53	761	181	1.11
29		551	468	242	76	40	113,700	1762	1075	1408	349	1.00
34		881	771	246	95	64	116,500	2925	1225	1511	825	1.39
27		1155	523	240	26	0	119,500	3960	3370	3730	99	1.04
45		1178	535	254	25	6	112,500	3780	2880	3486	102	1.06
23		1220	606	246	30	11	117,000	4140	3550	3710	173	1.07
39		1378	650	96	25	0	112,500	1680	43	1615	101	1.10
54		1430	441	91	17	0	110,000	1565	1007	1630	45	0.93
31		1500	551	96	19	0	117,000	1977	1017	1660	72	1.15
55		935	671	96	30	0	119,000	1280	535	1092	144	1.04
37		935	716	98	30	0	111,800	1148	597	983	134	1.03
60	*	447	447	242	280	219						
30	*	507	441	246	285	221						
47	*	724	695	85	104	80						
40	*	729	624	92	116	61						
56		870	835	100	78.5	37.8						
43		1080	750	94.5	28.4	0						
36		1287	420	98.3	18.9	0						
49		782	620	241	60.5	34						
33		835	642	244	37.8	15.1						
48		814	716	246	56.7	11.3						
25		606	578	241	64.3	23.6						
61		551	408	246	229	169						

TABLE III
DATA FROM DYNAMIC TESTS OF ULTRACAL 60, SERIES I (Cont.)

Specimen Number	Not Fractured First Tensile Phase	t_1 (10^{-6} in./in.)	t_2 (10^{-6} in./in.)	t_3 (10^{-6} sec)	t_4 (10^{-6} sec)	t_5 (10^{-6} sec)	c (in./sec)	$\frac{M_1}{P}$ (in. ² /sec)	$\frac{M_2}{P}$ (in. ² /sec)	$\frac{M_3}{P}$ (in. ² /sec)	$\frac{M_4}{P}$ (in. ² /sec)	$\frac{M_1 - M_4}{M_3}$
52		584	496	238	77.5	56.7						
38		706	578	259	106	75.6						
44		752	636	94.5	98.4	73.6						
24		1970	406	100	24.6	0						
58		671	430	488	87.5	68.5						
57		561	441	490	217	190						
50		606	606	484	274	190						
51		606	441	810	64.6	34.2						
32		484	441	802	103	68.4						
41		467	311	484	121	76						

would be expected to be slightly larger than unity, because $M_1 - M_4$ includes momentum of fragments broken off between the first fracture and strain gage, whereas M_3 does not.

Since time of breaking the silver strip was not a valid measure of time of fracture, it was decided that strain gages would be placed as close as possible to the section which first reached maximum tension and at which the first fracture was most likely to occur in all following series of tests.

b. Ultracal 60 Series 2

Data from this series of experiments are presented in table IV. A plot of strain magnitude vs. strain duration is presented in figure 21. The plaster mixture and method of preparing specimens were identical to the previous series except that an attempt was made to place strain gages at the section which would first be subjected to maximum tension.

Maximum tensile stress observed in the specimens was about 3.75 times the mean static tensile strength, and about 2.65 times the highest observed static tensile strength.

At a tensile strain of 433 microinches per inch (the mean static ultimate strain plus two standard deviations), 97.7 percent of specimens would be fractured in static tests, but no specimens were fractured in dynamic tests in which duration of load was less than 100 microseconds.

The longest duration of loading in this series of experiments was about 260 microseconds. Note that for an appreciable number of specimens, as seen in figure 20, fracture did not occur during the first tensile phase. In these cases, the strain pulse continued to travel back and forth in the specimen for an unknown number of cycles before fracture actually was completed.

Martin and Murphy¹¹ defined a quantity, K , which in the notation of this report can be written as

$$K = \int_0^{t_4} \left[\frac{\epsilon - \epsilon_s}{\epsilon_s} \right] dt$$

Values of K were computed for tests in which average pulse duration was less than 80 microseconds. For this series, the standard deviation of K was 19.3 percent of the mean, whereas standard deviation of static tensile strength was 20.5 percent of the mean. However, values of K for average pulse durations greater than 80 microseconds were more variable. It

appears that K is a good measure of resistance to dynamic fracture of this material for pulse durations below 80 microseconds, but much less good for pulses of longer duration.

c. Hydrostone

Data for experiments with Hydrostone are presented in table V. A plot of strain magnitude vs. strain duration is presented in figure 21.

The highest tensile stress in Hydrostone was about 2.65 times the static mean value and about 1.94 times the highest static value. At these values of stress, specimens were breaking before the tensile stress could reach its maximum value, that is, the magnitude of the incident compressive pulse. When pulse durations were as long as 400 microseconds, stress required to break specimens was still significantly above the static value.

Hydrostone was mixed in a vacuum, with degassed water, and had virtually no voids visible to the unaided eye. Ultracal 60, on the other hand, was mixed in a flat pan with a trowel, and under 10 power magnification showed many evenly distributed small voids. The hydrostone exhibits appreciably more scatter in data, particularly at the higher loading intensities and shorter load durations.

d. Portland Cement Mortars

Data from tests on specimens of portland cement mortar are presented in tables VI and VII. A plot of strain magnitude vs. strain duration is presented in figures 22 and 23.

The highest tensile stress recorded in dynamic tests was about 2.57 times the static mean tensile strength and about 1.77 times the highest observed static tensile strength.

It appears that these dry portland cement mortars, made with Ottawa sand, will fracture at essentially the static fracture stress if load duration is in excess of 200 microseconds. When load duration is as short as 30 microseconds, stress must be about twice the static tensile strength if fracture is to occur.

Strain gages were placed somewhat further from the free end of specimens than the ideal location, i.e., the section first subjected to maximum tensile strain. As a consequence, it was necessary to adjust the values for strain duration $(t_4 + t_8)/2$, which occurred in the section which was first subjected to maximum tensile strain, to compensate for the gage location.

TABLE IV

DATA FROM DYNAMIC TESTS OF ULTRACAL 60, SERIES 2

Batch	Specimen Number	Age at Test (days)	Not Fractured First Tensile Phase	c (in./sec)	d ₂ (in.)	' ₂ (10 ⁻⁶ in./in.)	t ₃ (10 ⁻⁶ sec)	t ₄ (10 ⁻⁶ sec)	t ₈ (10 ⁻⁶ sec)	$\frac{t_4 + t_8}{2}$ (10 ⁻⁶ sec)	t ₉ (10 ⁻⁶ sec)	$\frac{KS}{pc^2}$ (10 ⁻⁹ sec)
23	62	38		114,700	5.8	1160	118	18	10	14	8	11.0
	63	39		113,200	6.7	1155	114	22	14	18	8	14.6
24	65	39		113,800	6.6	903	114	60	44	52	8	29.2
	66	39		115,000	7.4	722	116	44	34	39	12	15.4
	67	33		-	-	560	280	164	132	148	24	35.2
25	68	27		113,000	17.3	593	276	156	120	136	20	37.0
	69	35		113,800	6.1	621	120	54	44	49	10	14.8
	70T1	36	*	113,500	-	508	118	120	64	92	16	-
	70T2	36	*	-	-	565	116	121	82	102	14	23.4
	71T1	30	*	110,500	-	517	260	280	212	246	24	47.4
	71T2	30	*	-	17.2	539	268	282	216	249	20	53.3
26	72T1	30	*	-	-	345	280	280	200	240	20	7.75
	72T2	30	*	108,600	-	432	276	280	224	252	8	29.0
	73T1	29	*	-	-	410	280	280	220	250	28	23.5
	73T2	29	*	115,000	8.1	485	276	280	240	260	12	44.0
27	74	24		114,400	11.8	572	276	156	120	138	20	33.9
	76	31		108,300	16.6	669	268	52	42	47	8	15.2
	77	30		115,000	-	518	276	224	172	198	16	38.6
	79	34		121,000	7.0	625	120	40	28	34	8	9.9
	80AT1	35	*	114,800	-	442	112	120	80	100	10	-
	80AT2	35		-	-	485	112	96	76	86	10	14.2
	80B	35		113,600	7.0	485	114	114	80	97	14	15.3
28	82	29	*	102,500	-	475	276	260	224	242	24	38.6
	83A	35	*	111,000	-	476	116	120	80	100	14	14.7
	84	36		112,200	7.4	608	120	52	32	42	16	11.1
29	86	30		108,300	5.8	680	276	128	88	108	20	36.9
	87	30		108,300	16.9	593	276	104	76	90	20	23.8
	88	36		116,200	-	618	116	126	90	108	12	30.8
	88A	36		114,200	-	654	118	104	80	92	10	29.8
	89	37		110,500	11.5	553	284	148	116	132	10	30.2
	90	36		113,200	6.6	700	116	50	30	40	10	14.2

TABLE V

DATA FROM DYNAMIC TESTS OF HYDROSTONE

Batch	Specimen Number	Age at Test (days)	Not Fractured First Tensile Phase	c (ln./sec)	d ₂ (ln.)	$\dot{\epsilon}_2$ (10^{-6} ln./ln.)	$\dot{\epsilon}_3$ (10^{-6} sec)	$\dot{\epsilon}_4$ (10^{-6} sec)	$\dot{\epsilon}_6$ (10^{-6} sec)	$\frac{\dot{\epsilon}_4 + \dot{\epsilon}_6}{2}$ (10^{-6} sec)	$\dot{\epsilon}_9$ (10^{-6} sec)	$\frac{K_5}{pc^2}$ (10^{-9} sec)
2	2EA 2EB	56 56		114,000	6.0 6.2	619 946	117 119	21 39	9 17	15 28	9 10	12.5
3	4H 5H	40 40		118,400	- 9.7	506 662	272 282	93 100	60 74	76 87	19 16	6.2
4	6H 7H	37 37		124,200	17.7 11.2	765 560	270 278	68 189	36 170	52 185	20 18	15.6
5	8HT1 8HT2 9H	36 36 37	* * *	122,300	- - 17.7	600 638 623	276 276 275	278 284 283	220 237 224	249 260 253	18 18 12	-
6	10HA 10HB 11H	36 36 41		122,400	6.9 - 31.8	874 808 548	112 112 516	51 35 244	20 13 206	35 24 225	14 10 10	12.6 7.4
7	12HT1 12HT2 13HAT1 13HAT2 13HB	41 41 37 37 37	* * * * *	124,000	- 30.2 - - 3.6	623 646 710 710 670	510 512 120 120 118	414 80 120 120 118	322 54 82 82 82	368 67 101 101 100	16 10 12 12 10	-
8	14HA 14HB 15H 16H	37 37 41 41	* * * *	125,200	4.6 9.3 7.5 18.6	749 630 584 567	118 118 270 272	80 120 230 132	56 78 184 76	68 99 207 104	12 14 22 40	21.0
9	17H 18H 19H	35 34 42		124,200	- 7.1 -	804 746 717	260 278 252	64 276 236	20 212 210	42 244 223	32 20 16	12.3
10	20H 21H 22H	41 38 38		121,800	14.4 - 5.9	717 763 678	266 276 280	209 140 204	164 88 164	186 114 184	24 24 20	-
12	23H 24H	41 71	*	119,000	13.5 -	642 520	269 510	264 352	224 326	244 339	18 24	-

TABLE IV
DATA FROM DYNAMIC TESTS OF ULTRACAL 60, SERIES 2 (Cont.)

Batch	Specimen Number	Age at Test (days)	Not Fractured Prior to Failure Phase	σ (lb./sq.)	d_2 (in.)	t_2 (10^{-6} in./in.)	t_3 (10^{-6} sec)	t_4 (10^{-6} sec)	t_5 (10^{-6} sec)	$\frac{t_4 + t_5}{2}$ (10^{-6} sec)	t_9 (10^{-6} sec)	$\frac{K_2}{pc^2}$ (10^{-9} sec)
30	91	37		107,300	6.3	621	260	180	148	164	20	49.0
	92	30		107,300	-	647	280	89	60	74	20	22.8
31	94	29		114,500	15.4	658	260	64	24	44	16	12.3
	95	36		113,300	-	640	276	282	200	241	32	73.5
	96T1	36		118,300	-	587	272	276	220	248	24	65.3
	96T2	36		-	-	576	264	128	88	108	24	26.0
	97A	35		115,100	-	695	110	32	18	25	10	13.5
	97B	35		119,100	-	648	116	74	60	67	16	21.8
	98A	35		105,000	6.7	903	112	38	18	28	14	14.9
32	98B	35		120,300	5.8	587	116	60	46	53	12	14.2
	99	36		108,300	16.6	542	260	88	52	70	24	14.1
	100	35		111,000	6.3	848	110	24	14	19	12	9.2
	101	33		110,000	-	858	110	30	20	25	10	12.7
	102	33		113,800	7.5	722	110	48	30	39	6	14.5
	103	36		111,300	18.9	677	268	200	140	170	32	57.7

TABLE V

DATA FROM DYNAMIC TESTS OF HYDROSTONE (Cont.)

Batch	Specimen Number	Age at Test (days)	Not Fractured Prior to Test	σ (lb./sq.in.)	d_2 (in.)	t_2 (10^{-6} in./in.)	t_3 (10^{-6} sec)	t_4 (10^{-6} sec)	t_8 (10^{-6} sec)	$\frac{t_4 + t_8}{2}$ (10^{-6} sec)	t_9 (10^{-6} sec)	$\frac{KS}{pc^2}$ (10^{-9} sec)
25	53H 54HB 55HA	37 45 49		122,300	14.7 - -	709 789	270 110	96 48	62 26	79 37	18 10 9	20.8 11.9
26	56H 57H 58H	35 35 35	*	124,200	- 16.9 20.6	650 753 697	270 268 269	175 78 272	144 46 223	160 62 248	18 16 16	- 18.4 -
27	59H 60H	35 35		127,200	9.6 14.7	796 768	270 272	121 81	90 50	105 65	16 12	- 20.5
28	61H 62HT1 62HT2 63H	35 35 35 35	* * * *	123,600	15.7 - - 15.3	658 646 776 721	267 268 268 264	272 272 272 50	310 222 218 28	241 247 245 39	20 16 20 14	- - - 10.3
29	64HT1 64HT2 65H	28 28 28	*	123,400	- 27.6 -	638 725 631	516 516 516	432 222 100	364 166 44	398 194 72	24 36 32	- - 12.1
30	67HT1 67HT2 67HT3	59 59 59	* * *	125,600	- - -	647 680 684	512 512 512	428 436 376	362 364 324	398 400 350	32 40 36	- - -
31	68H 69HA	59 40	*	126,100	- 5.6	670 945	504 116	438 80	380 50	409 65	24 25	- 31.4
32	70H 71H	55 55	* *	122,300	- 19.3	693 670	504 504	424 420	362 358	393 389	28 24	- -
33	72H 73H	55 55		124,000	25.3 -	705 616	504 504	348 100	304 78	326 89	20 20	- -
35	74HA 75H	31 54	*	125,000	6.9 32.7	793 710	112 504	43 438	25 374	34 406	10 32	11.3 -
36	76H 77H	55 55		122,300	31.7 -	642 666	512 512	62 212	36 172	49 192	20 24	9.6 -

TABLE V

DATA FROM DYNAMIC TESTS OF HYDROSTONE (Cont.)

Batch	Specimen Number	Age at Test (days)	Not Fractured First Penetration Phase	c (in./sec)	d_2 (in.)	a_2 (10^{-6} in./in.)	t_3 (10^{-6} sec)	t_4 (10^{-6} sec)	t_6 (10^{-6} sec)	$\frac{t_4 + t_6}{2}$ (10^{-6} sec)	t_7 (10^{-6} sec)	$\frac{KS}{PC^2}$ (10^{-9} sec)
14	26H 28H	41 41		125,800	20.9 19.4	709 804	270 270	256 208	212 172	234 190	18 18	-
15	29H 30H 31H	41 41 40		125,100	9.0 15.9 19.2	674 749 697	267 270 268	157 58 99	123 32 57	140 4.5 78	18 16 18	- - 19.1
16	32HT1 32HT2 32HT3 33HA	70 70 70 50	* * *	116,800	- - - 7.8	543 583 630 776	506 516 516 115	436 430 432 35	368 368 358 17	402 399 395 26	32 28 32 10	- - - 7.8
17	34H 35H	41 70		116,300	8.7 16.8	631 650	272 510	132 256	118 220	125 238	18 20	-
18	36H 37H 38H	41 41 41		123,700	17.7 17.7 -	725 697 846	268 267 272	60 121 172	30 92 60	45 106 116	18 20 95	10.7 -
19	39H 40H	41 36		120,700	- 31.5	682 465	264 516	100 62	68 0	84 31	18 31	-
20	41H 42H	40 35	*	121,900	- 14.3	729 646	270 524	270 224	218 164	244 194	18 28	-
21	43H 44HT1 44HT2 45H	40 40 40 41	*	122,800	- - - 20.1	645 741 623 745	271 269 270 270	223 278 62 112	192 225 29 65	207 251 46 88	18 14 12 16	-
22	46H 47H	41 36		123,300	6.3 -	713 638	268 516	230 290	158 236	214 263	18 36	-
23	49H	35			-	612	516	200	142	171	28	-
24	50H 51H 52HB	41 41 48	*		- 9.8 8.8	725 726 790	268 272 112	275 170 60	245 132 39	260 151 50	18 20 10	- - 17.2

TABLE V

DATA FROM DYNAMIC TESTS OF HYDROSTONE (Cont.)

Batch	Specimen Number	Age at Test (days)	Not Fractured First Tensile Phase	σ (ln./sec)	d_2 (ln.)	t_2 (10^{-6} ln./ln.)	t_3 (10^{-6} sec)	t_4 (10^{-6} sec)	t_6 (10^{-6} sec)	$\frac{t_4 + t_6}{2}$ (10^{-6} sec)	t_9 (10^{-6} sec)	$\frac{K_3}{pc^2}$ (10^{-9} sec)
46	99H	10		123,700	7.2	501	270	170	142	156	16	-
	100HA	31			6.9	950	111	30	11	20	10	8.5
	101H	10		122,900	-	721	270	116	92	104	16	-
47	102H	9	*		7.5	662	266	268	210	239	18	-
	103H	9		127,500	18.2	614	268	76	42	59	18	9.8
	104HA	16			10.3	694	116	84	36	60	34	13.1
	104HB	30			-	977	111	25	13	19	10	9.4
48	105HA	28			7.2	749	109	31	17	24	10	6.9
	105HB	28			8.7	907	112	40	25	32	9	14.2
	106HA	28		128,100	6.1	1086	114	31	5	18	20	8.9
	106HB	28			6.8	937	111	30	10	20	11	8.3
	107HA	28			10.1	937	110	45	12	29	24	11.6
49	107HB	28			7.8	741	109	39	21	30	9	8.3
	108HA	23		125,000	10.4	953	112	59	39	49	10	24.4
	108HB	23			7.8	938	111	49	26	37	10	17.1
	109HA	23			10.6	716	114	81	23	52	35	10.9
	109HB	23			5.8	678	114	58	26	42	34	8.8
	110HA	23			7.5	733	112	42	22	32	11	8.6
	110HB	23			9.1	773	112	48	22	35	11	10.5

TABLE V

DATA FROM DYNAMIC TESTS OF HYDROSTONE (Cont.)

Batch	Specimen Number	Age at Test (days)	Not Fractured First Tensile Phase	C (ln./sec)	d ₂ (ln.)	t ₂ (10 ⁻⁶ ln./ln.)	t ₃ (10 ⁻⁶ sec)	t ₄ (10 ⁻⁶ sec)	t ₆ (10 ⁻⁶ sec)	$\frac{t_4 + t_6}{2}$ (10 ⁻⁶ sec)	t ₉ (10 ⁻⁶ sec)	$\frac{KS}{\rho C^2}$ (10 ⁻⁹ sec)
37	78H 79H	54 54		122,200	15.2 31.4	618 631	502 508	246 336	192 312	219 324	20 20	- -
39	80H 81H	53 53		127,200	31.5 21.4	560 627	504 512	60 400	18 352	39 376	20 20	- -
40	82HT1 82HT2 83HB 84HA 84HB	18 18 31 31 31	*	126,100	- 20.7 9.1 6.4 9.8	544 705 899 591 906	259 265 112 113 112	270 180 53 50 81	289 142 33 26 41	245 161 43 38 61	16 22 10 8 20	- - 18.9 5.4 25.9
41	86HB 87HA 87HB 88HA 88HB	31 31 31 31 31		127,400	8.8 5.6 8.2 8.1 8.8	685 790 887 844 1025	112 113 112 112 111	55 44 45 49 50	32 20 23 26 29	44 32 34 39 40	10 9 10 10 11	10.4 9.9 13.7 14.7 22.0
42	89HB 90HB 91HA	30 30 30		121,400	6.8 6.8 6.5	914 930 702	113 112 113	40 29 30	15 14 14	28 21 22	11 10 9	11.4 9.1 5.1
43	92HB 93HA 93HB	34 34 34		125,000	7.1 7.2 8.3	915 1030 788	114 113 112	27 38 46	9 18 32	18 28 39	9 11 10	7.1 14.9 13.5
44	94HA 94HB 95HB	33 33 33		128,800	5.9 8.4 7.4	638 738 836	111 112 112	55 40 30	39 22 10	47 31 20	10 9 9	9.6 8.6 6.5
45	96HA 96HB 97HA 97HB 98HA 98HB	36 36 36 36 36 36		122,700	10.0 7.2 7.8 7.5 7.5 7.5	638 930 1068 934 970 954	111 114 112 113 112 113	79 34 39 40 36 32	56 17 22 23 10 12	68 25 31 31 23 22	8 9 10 9 20 10	14.0 11.0 18.2 14.5 9.8 9.7

BLANK PAGE

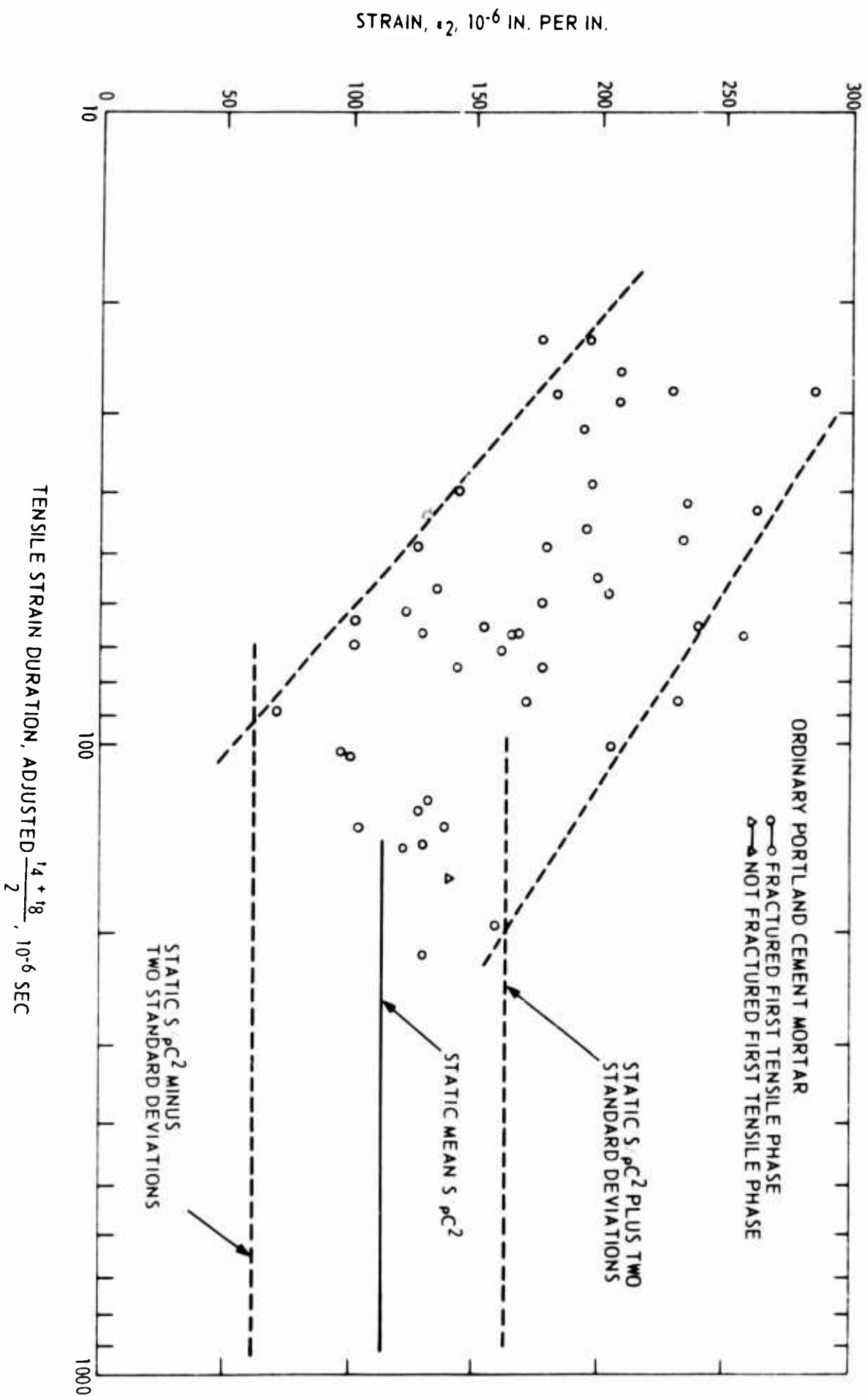


Figure 23. Strain Magnitude vs. Strain Duration for Ordinary Mortar

Tables VI and VII present these adjusted values which were calculated on the basis of strain gage location, first fracture, the section first subjected to maximum tension, and the rise time of the strain pulse.

e. Application

Information obtained in this investigation is believed to have practical applications in any situation in which the materials tested are to be fractured in tension, at or near atmospheric pressure, by stresses applied very rapidly. Situations in which this type of fracture is predominant include percussion drilling, demolition of concrete structures, and prediction of fracture due to large explosions by observing fracture in small-scale model explosions. It is dangerous to extrapolate results of tests on these materials to rocks, etc., for which no experimental data exists. However, it seems reasonable to assume that some rocks will exhibit behavior similar to the materials tested.

Reichmuth¹ has established that the most significant mode of rock fracture in percussion drilling is tensile fracture. Information of the type obtained in this investigation should be valuable in selecting or designing percussion drills for drilling in a particular type of rock in order to minimize energy expended in drilling. The energy that must be supplied to the striker of a percussion drill is equal to one-half its mass multiplied by the square of its velocity. Duration of impulse is proportional to striker length, and strain magnitude is proportional to striker velocity.

Some values of pulse duration, strain magnitude and energy of pulse required to produce fracture of Ultracal 60 are given in table VIII. Combinations of pulse duration and strain magnitude were taken from the upper bound to the experimental data in figure 20. It is seen that a pulse duration of 40 microseconds at 800 microinches per inch resulted in fracture with significantly less expenditure of energy than longer pulses of lesser magnitude. Increasing strain magnitude did not materially reduce energy required to complete fracture.

A closely analogous situation may exist in percussion drilling. Certain combinations of striker length and velocity may produce maximum drilling efficiency in a particular rock, while a longer striker wastes energy and higher impact velocity produces unnecessary wear on striker and drill steels.

Applications of data of the type generated in this investigation to the design of demolition and small-scale blasting procedures is direct and obvious. Of course, it is necessary that experimental data be available for the type of material to be blasted. Also, data must be available on intensity and duration of strain pulses produced by various explosive charges. The principle that

TABLE VI

DATA FROM DYNAMIC TESTS OF HIGH EARLY STRENGTH PORTLAND CEMENT MORTAR

Batch	Specimen No.	Not Fractured First Tensile Phase	c (in./sec)	d ₂ (in.)	t ₂ (10 ⁻⁶ in./in.)	t ₃ (10 ⁻⁶ sec)	t ₄ (10 ⁻⁶ sec)	t ₅ (10 ⁻⁶ sec)	$\frac{t_4 + t_5}{2}$ (10 ⁻⁶ sec)	t ₉ (10 ⁻⁶ sec)	Compressive Phase Rise Time (10 ⁻⁶ sec)	$\frac{t_4 + t_5}{2}$ (10 ⁻⁶ sec)	$\frac{KS}{pc^2}$ (10 ⁻⁹ sec)
13	33CB T1 33CB T2	*	161,800	--	152 174	129 124	133 146	88 80	110 113	20 20	25 24	-- 104	-- 4.29
14	36CB 38CA 38CB		162,200 162,000 154,800	8.7 -- 13.5	216 185 152	124 119 120	57 119 80	30 79 52	44 99 66	15 16 15	20 18 20	44 -- 82	3.42 -- 2.20
15	40C 41C 42C		171,000 150,300 159,800	25.2 -- 23.7	153 201 190	280 287 289	75 68 113	42 18 80	69 43 82	15 24 40	24 36 52	144 -- 107	4.18 -- 5.52
16	44C 45C		169,200 157,200	18.4 21.6	199 156	292 306	180 138	130 90	185 114	36 32	50 48	142 113	9.90 3.29
17	46C 48C		153,000 161,900	29.9 23.4	96 141	303 283	140 95	90 60	115 77	30 20	44 24	146 105	-- 1.80
18	50C 51C 52C		164,500 167,800 154,500	23.0 26.1 --	170 179 195	303 280 280	197 147 197	62 110 163	130 129 189	110 22 10	46 30 16	147 163 --	4.85 8.70 --
19	53C 55C 56C	*	163,300 161,000 156,800	-- 29.8 --	163 141 170	283 318 281	260 228 281	217 80 228	239 154 285	26 130 28	28 140 20	-- 141 --	-- 1.56 --
20	57C 58C 60C		169,000 159,700 153,500	25.8 23.6 26.1	130 220 143	302 283 288	165 90 202	122 42 30	144 66 116	28 32 152	50 42 46	175 93 147	1.38 7.92 1.63
21	62C 63C 64C		158,200 164,500 174,300	29.4 -- 21.0	129 167 156	306 296 300	160 210 128	82 147 50	121 179 89	72 36 60	62 40 50	148 -- 81	0.89 -- 1.89
22	66C 65C 67C 68C		173,800 169,000 148,000 165,600	21.0 -- 22.9 22.7	150 173 170 166	300 282 292 292	280 241 188 219	220 203 119 163	260 222 153 191	30 24 32 32	50 32 58 44	242 -- 166 204	6.32 -- 6.91 8.28

TABLE VII

DATA FROM DYNAMIC TESTS OF ORDINARY PORTLAND CEMENT MORTAR

Batch	Specimen No.	Not Fractured First Tensile Phase	σ (lb./sq.)	d_2 (in.)	t_2 (10^{-6} in./in.)	t_3 (10^{-6} sec)	t_4 (10^{-6} sec)	t_5 (10^{-6} sec)	$\frac{t_4 + t_5}{2}$ (10^{-6} sec)	t_9 (10^{-6} sec)	Compressive Phase Rise Time (10^{-6} sec)	$\frac{t_4 + t_5}{2}$ Adjusted (10^{-6} sec)	$\frac{KS}{2}$ pc (10^{-9} sec)
24	73CB		146,200	7.5	99	136	116	68	92	22	50	105	3.76
	74CA		145,500	11.4	177	140	98	34	66	30	60	76	
	74CB		152,100	12.2	199	119	59	12	36	32	24	55	
	75CA		140,000	8.9	195	118	52	19	35	24	24	39	
	75CB		150,400	9.2	207	124	30	10	20	16	22	29	
25	76CA		155,200	8.6	183	128	48	7	28	22	30	28	1.08
	76CB		147,400	8.0	195	128	41	20	30	18	28	23	
	77CA T1	•	145,800		216	125	102	16	59	20	34	--	
	77CA T2		120,900	8.8	100	96	70	50	60	10	22	64	
	77CB		145,800	13.4	170	124	106	36	71	28	38	86	
27	78CA		141,100	8.8	227	123	42	7	25	22	24	28	3.72
	78CB		150,100	17.5	232	120	50	16	33	28	42	48	
	79CA		150,800	8.3	285	120	58	11	35	32	40	28	
	79CB		144,900	12.5	125	120	39	18	29	18	20	49	
	80CA		160,100	12.5	202	119	61	21	41	20	32	58	
28	80CB		144,300	9.2	142	122	52	10	31	14	13	40	4.27
	85CA		145,100	11.4	286	114	64	30	47	18	14	68	
	85CB		160,000	12.2	160	123	66	38	52	12	24	71	
	86CA		166,800	--	162	120	122	80	101	22	30	--	
	86CB		170,100	8.7	192	120	60	30	45	14	28	46	
29	87CA		166,100	12.3	176	119	52	28	40	16	20	60	3.38
	87CB		180,000	11.6	204	119	102	60	91	20	18	101	
	88CA		161,000	12.5	120	130	66	29	47	18	40	62	
	88CB		161,000	8.6	177	115	74	21	48	30	24	49	
	89CA		144,300	10.5	262	121	44	6	25	28	30	43	
30	89CB		140,200	8.1	208	130	53	17	35	22	36	26	1.55
	90CA		147,300	11.7	228	128	76	18	47	32	24	66	
	90CB		130,000	12.0	164	110	100	10	55	48	48	68	
	91CA		154,000	11.7	230	121	88	46	67	20	26	86	
	91CB		140,100	10.8	100	132	80	24	52	40	28	70	
31	92CA		140,000	11.3	142	123	90	26	58	28	26	76	1.58

TABLE VI

DATA FROM DYNAMIC TESTS OF HIGH EARLY STRENGTH PORTLAND CEMENT MORTAR (Cont.)

Batch	Specimen No.	Not Fractured First Tensile Phase	c (in./sec)	d ₂ (in.)	t ₂ (10 ⁻⁶ in./in.)	t ₂ (10 ⁻⁶ sec)	t ₄ (10 ⁻⁶ sec)	t ₈ (10 ⁻⁶ sec)	$\frac{t_4 + t_8}{2}$ (10 ⁻⁶ sec)	t ₉ (10 ⁻⁶ sec)	Compressive Phase Rise Time (10 ⁻⁶ sec)	$\frac{t_4 + t_8}{2}$ Adjusted (10 ⁻⁶ sec)	$\frac{KS}{pc^2}$ (10 ⁻⁹ sec)
23	70CA		152,500	11.6	168	136	94	36	65	44	40	71	2.35
	70CB		166,300	10.7	206	136	92	24	88	44	54	66	3.91
	71CA		163,900	11.6	93	128	100	46	74	10	32	87	--
	71CB		164,800	8.3	122	130	128	83	106	20	28	98	0.08
	72CA		146,000	9.3	158	124	96	83	75	16	20	83	2.44
	72CB		166,800	10.4	222	126	73	31	52	22	24	67	5.65
26	81CA		138,600	11.6	182	125	80	14	47	20	60	53	1.89
	81CB		143,100	9.9	253	126	39	13	26	20	28	39	4.36
	82CA		149,500	--	224	122	56	22	39	20	20	--	--
	83CA		141,500	11.7	199	136	74	39	56	24	36	68	4.45
	83CB		150,900	11.8	158	130	60	46	60	10	20	66	2.15
	84CA		148,200	5.0	159	127	118	80	99	20	24	93	3.00
	84CB		152,000	11.4	125	126	95	50	72	16	62	78	--
29	93CB		162,500	8.2	267	126	51	28	40	16	26	34	4.23
	94CA		161,900	6.5	258	121	62	28	45	18	26	39	4.24
	94CB		159,500	11.7	250	121	56	36	47	12	20	63	--
	95CA		161,900	11.5	232	120	52	20	36	18	22	52	4.88
	95CB		159,500	8.2	209	121	70	43	67	18	20	53	3.96
	96CA	*	150,600	10.8	148	121	122	40	81	20	25	96	1.70

TABLE VII

DATA FROM DYNAMIC TESTS OF ORDINARY PORTLAND CEMENT MORTAR (Cont.)

Batch	Specimen No.	Not Fractured First Resonance Phase	σ (lb./sq.)	d_2 (in.)	t_2 (10^{-6} in./in.)	t_3 (10^{-6} sec)	t_4 (10^{-6} sec)	t_5 (10^{-6} sec)	$\frac{t_4 + t_5}{2}$ (10^{-6} sec)	t_9 (10^{-6} sec)	Compressive Phase Time (10^{-6} sec)	$\frac{t_4 + t_5}{2}$ Adjusted (10^{-6} sec)	$\frac{K_2}{pc^2}$ (10^{-9} sec)
30	97C		160,000	25.8	120	280	146	70	108	80	44	140	1.02
	99C		160,000	--	190	280	120	24	72	30	--	--	
31	101C		150,000	27.0	128	260	150	60	105	72	--	145	1.24
	102C		157,100	20.4	96	276	160	60	110	52	38	104	
	103C		162,000	--	98	284	182	122	152	60	32	--	
	104C		162,200	--	90	271	142	48	95	70	30	--	
32	106C T1	*	155,000	--	107	208	204	175	240	44	60	--	
	106C T2	*	150,000	25.6	180	205	197	118	154	40	40	105	8.15
	107C T1	*	152,200	20.8	140	205	215	106	200	50	42	262	6.12
	107C T2		157,200	--	181	210	82	26	54	24	--	--	
	108C T1	*	162,200	--	104	201	200	200	200	46	40	--	
	108C T2		160,000	16.8	120	209	246	125	190	24	24	200	2.58
33	109C T1		160,700	--	120	205	200	202	241	50	40	--	
	109C T2		160,000	22.6	--	208	90	--	--	--	42	--	
	110C	*	156,000	10.8	126	224	282	0	141	22.2	50	128	0.06
34	111C		158,500	22.8	167	200	82	18	80	42	24	67	2.58
	112C		157,500	22.2	122	202	66	17	42	22	50	57	0.79
	114C		150,700	20.1	60	200	72	17	45	22	20	89	
	115C		156,000	10.2	127	208	114	20	75	50	24	67	0.51
35	116C		152,500	16.9	152	200	124	24	79	66	54	66	1.01
	117C		157,000	21.0	128	200	172	90	125	52	40	127	2.89
	119C		154,000	--	197	202	190	102	146	40	--	--	
	120C		151,200	21.0	120	202	146	77	111	50	--	124	1.79
36	121CB		154,000	0.9	222	122	56	18	37	24	20	42	4.03
	122CA		162,000	7.9	178	122	40	10	20	14	26	22	1.02
	122CB		146,000	5.5	186	120	56	19	37	10	22	22	1.57
	123C		161,000	10.7	102	272	100	100	144	54	22	120	--
	124C		140,000	--	128	210	210	56	122	120	74	--	--

TABLE VIII

ENERGY ASSOCIATED WITH FRACTURE OF ULTRACAL 60

Pulse Duration (10^{-6} sec)	Strain (10^{-6} in./in.)	Energy of Pulse (arbitrary units)
200	680	924
100	700	490
40	800	256
20	1120	250

has been established is that increasing duration of explosive loading is sometimes interchangeable with increasing intensity of explosive loading in accomplishing more effective demolition.

Information of the type generated by this investigation is essential if fracturing by large explosions is to be predicted by observation of small-scale model explosions. Small-scale model experiments have been made by Johnson,⁹ Martin,¹⁸ and Kochanowsky and Pinto.¹⁹ As discussed by Martin and Murphy,¹¹ there is good evidence that scale-model blasts, employing the same explosive and the same resistant material, and of similar geometry, result in the same strain magnitudes at equivalent locations as in large blasts. However, all times are reduced in the same proportion as the length scale of the model.

It is evident from figure 20 that an explosive loading on Ultracal 60 with pulse duration of 200 microseconds and magnitude of 700 microinches per inch, would cause complete fracture. However, in a one-tenth scale model, with pulse duration of 20 microseconds and magnitude of 700 microinches per inch, no fracture would occur. This comparison is a bit oversimplified because strain pulses from explosions are not exactly of the same shape as the pulses generated in this investigation, but the comparison is certainly valid in principle.

On the other hand, data plotted in figures 22 and 23 indicate that mortars completed fracture within 200 microseconds even at the strain levels associated with static tests. Consequently, models made of these materials would probably give good indications of fracture in large systems, provided tensile strain duration in the model was appreciably longer than 200 microseconds.

BLANK PAGE

SECTION 5

CONCLUSIONS

Dynamic fracture behavior of the high-strength gypsum plaster, low-strength gypsum plaster, high early strength portland cement mortar, and ordinary portland cement mortar tested were qualitatively similar. In each case, as strain magnitude increased, time required to complete fracture decreased.

Strain required to break plaster was significantly above the static fracture value at the longest loading durations (about 400 microseconds). Mortars broke at the static fracture strain after load had existed for about 200 microseconds.

The quantity

$$K = \int_0^t \left[\frac{\epsilon - \epsilon_s}{\epsilon_s} \right] dt$$

defined by Martin and Murphy,¹¹ appeared to be a good measure of resistance to dynamic fracture of low-strength gypsum plasters at load durations of less than 80 microseconds. For other materials and longer load durations, the standard deviation of K was a larger percentage of its mean value than was the case for static tensile strength.

Tensile fracture of these materials cannot be predicted by specifying a fracture stress or fracture strain if load is applied rapidly, as in these experiments.

It appears that sections of natural rock drill cores could be glued together with Eastman 910 cement to make long bars suitable for dynamic testing of the type used in this investigation.

Measurement of time at which current ceased to flow through silver strips painted on specimens was not an adequate measure of time at which fracture occurred.

The special loading machine constructed by Melpar was, in general, quite successful.

Casting of long bar test specimens was difficult. In future work, consideration should be given to dynamic test specimens of rectangular or

triangular cross section. Such work is necessary to determine variations due to sample configurations and, at the same time, long specimens should be easier to obtain in rectangular shapes.

Additional experimental work should be done to determine whether other materials exhibit behavior similar to those already tested. In particular, tests should be made on portland cement mortars with aggregates other than Ottawa sand and on natural rock cores as well as concrete (in determining the behavior of structures).

In future experiments employing the technique used in this investigation, specimens should be pre-inspected by sending a low-amplitude pulse down the specimen and observing the reflection. This could disclose the presence of cracks or flaws in the specimen. Also, speed of sound in the specimen could be determined so that the strain gage could be placed exactly at the section which first will experience maximum tension.

Techniques for testing specimens with high moisture contents should be developed. It is suspected that time required to complete fracture is longer at high moisture contents.

More research is required to establish a general criterion or property for measuring resistance to fracture under dynamic loading.

REFERENCES

1. Reichmuth, D. R., Correlation of Force-Displacement Data with Physical Properties of Rock for Percussive Drilling Systems, 5th Symposium on Rock Mechanics, C. Fairhurst, Ed., Pergamon Press, 1963.
2. Clark, G. B. and R. D. Caudle, "Brittle Fracture of Small Short Rock Beams Under Central Transverse Impact Loading," 4th Symposium on Rock Mechanics, Bulletin, Mineral Industries Experiment Station, Pennsylvania State Univ., University Park, Pa., 1961, p. 137.
3. Martin, C. W., "Fracture of Plaster by Explosions." Dissertation in partial fulfillment of the requirements for the degree of Doctor of Philosophy, Iowa State University, Ames, Iowa, in 1962 (unpublished).
4. Nicholls, H. R., V. Hooker, and W. I. Duvall, "Dynamic Rock Mechanics Investigation, Project Cowboy," U.S. Bu. of Mines Applied Physics Research Lab., College Park, Md., 1960.
5. Duvall, W. I. and T. C. Atchison, "Rock Breakage by Explosives," Report of Investigations 5356, Bu. of Mines, U.S. Dept. of the Interior, Washington, D.C., 1957.
6. Duvall, W. I. and B. Petkof, "Spherical Propagation of Explosion-Generated Strain Pulses in Rock," Report of Investigations 5483, Bu. of Mines, U.S. Dept. of the Interior, Washington, D.C. 1959.
7. Rinehart, J. S., "On Fractures Caused by Explosions and Impacts," Quarterly of the Colorado School of Mines, Golden, Colo., October, 1960, Vol. 55, No. 4.
8. Broberg, K. B., Some Aspects of the Mechanism of Scabbing, International Symposium on Stress Wave Propagation in Materials, New York, N. Y., Interscience Publishers Inc., 1960.
9. Johnson, J. B., "Small Scale Blasting in Mortar," Report of Investigations 6012, Bu. of Mines, U. S. Dept. of the Interior, Washington, D.C., 1962.
10. Hino, K., Theory and Practice of Blasting, Nippon Kayaku Co., Ltd., Asa, Yamaguchi-Ken, Japan, 1959.
11. Martin, C. W. and Glenn Murphy, "Model Prediction of Fracture Due to Explosions," J. Eng. Mechanics Div., ASCE, April 1963.

12. Timoshenko, S. and J. N. Goodier, Theory of Elasticity, McGraw-Hill, 1951.
13. Kolsky, H., Stress Waves in Solids, Dover, 1963.
14. ASTM Designation C 305-59T Mechanical Mixing of Hydraulic Cement Pastes and Mortars of Plastic Consistency. ASTM Standards Part 9, 1964.
15. ASTM Designation C109-63, Compressive Strength of Hydraulic Cement Mortars (Using 2-In. Cube Specimens). ASTM Standards Part 9, 1964.
16. ASTM Designation C190-63, Tensile Strength of Hydraulic Cement Mortars, ASTM Standards Part 9, 1964.
17. ASTM Designation C496-64T, Splitting Tensile Strength of Molded Concrete Cylinders ASTM Standards, Part 10, 1964.
18. Martin, C. W., "Influence of Depth and Shape of Charge on Crater Formation in Plaster," thesis presented in partial fulfillment of the requirements for the degree of Master of Science, Iowa State University, 1959 (unpublished).
19. Kochanowsky, B. J. and J. Pinto, "Laboratory Blasting with Models," 4th Symposium of Rock Mechanics, Bulletin, Mineral Industries Experiment Station, Pennsylvania State Univ., University Park, Pa., 1961, p. 179.

Unclassified

Security Classification

DOCUMENT CONTROL DATA - R&D		
(Security classification of title, body of abstract and indexing annotation must be entered when the overall report is classified)		
1 ORIGINATING ACTIVITY (Corporate author) Melpar, Inc. Falls Church, Virginia		2a REPORT SECURITY CLASSIFICATION Unclassified
		2b GROUP
3 REPORT TITLE FRACTURE OF GYPSUM PLASTERS AND CEMENT MORTARS BY DYNAMIC LOADING		
4 DESCRIPTIVE NOTES (Type of report and inclusive dates) 8 June 1964 to 1 July 1965		
5 AUTHOR(S) (Last name, first name, initial) Martin, Charles W.		
6 REPORT DATE December 1965	7a TOTAL NO OF PAGES 88	7b NO OF REFS 19
8a CONTRACT OR GRANT NO AF29(601)-6420	9a ORIGINATOR'S REPORT NUMBER(S) AFWL-TR-65-140	
b. PROJECT NO 5710		
c Subtask 13.144	9b OTHER REPORT NO(S) (Any other numbers that may be assigned this report)	
d		
10 AVAILABILITY/LIMITATION NOTICES Distribution of this document is unlimited.		
11 SUPPLEMENTARY NOTES	12 SPONSORING MILITARY ACTIVITY Air Force Weapons Laboratory (WLDC) Kirtland AFB, New Mexico 87117	
13 ABSTRACT <p>An experimental study was made of influence of strain magnitude and strain duration on dynamic fracture in uniaxial tension of low-strength gypsum plaster, high-strength gypsum plaster, high early strength portland cement mortar, and ordinary portland cement mortar. Dynamic test specimens were circular cylindrical bars with diameters ranging from 0.9 to 1.2 inches and lengths ranging from 18 to 58 inches. Static test specimens 2 inches long were cut from the long bars. A special loading device, designed and constructed by Melpar, generated a compressive pulse by longitudinal impact of two metal bars and applied the pulse to one end of the dynamic test specimens. The compressive pulse was reflected at the free end of specimens as a tensile pulse and caused fracture in tension at a section near the middle.</p> <p>Time from zero strain to maximum tensile strain varied from 10 to 35 microseconds, and total duration of tensile strain varied from 20 to 430 microseconds with few exceptions. All materials withstood tensile strains two to three times the static fracture strain for short periods. The straining time required to cause fracture varied with strain magnitude.</p>		

Unclassified

Security Classification

14	KEY WORDS	LINK A		LINK B		LINK C	
		ROLE	WT	ROLE	WT	ROLE	WT
	Dynamic Fracture of Brittle Material Static Tensile Strength Load Duration Tensile Strain Compressive Strain Gypsum Plaster Cement Mortar						

INSTRUCTIONS

1. **ORIGINATING ACTIVITY:** Enter the name and address of the contractor, subcontractor, grantee, Department of Defense activity or other organization (*corporate author*) issuing the report.

2a. **REPORT SECURITY CLASSIFICATION:** Enter the overall security classification of the report. Indicate whether "Restricted Data" is included. Marking is to be in accordance with appropriate security regulations.

2b. **GROUP:** Automatic downgrading is specified in DoD Directive 5200.10 and Armed Forces Industrial Manual. Enter the group number. Also, when applicable, show that optional markings have been used for Group 3 and Group 4 as authorized.

3. **REPORT TITLE:** Enter the complete report title in all capital letters. Titles in all cases should be unclassified. If a meaningful title cannot be selected without classification, show title classification in all capitals in parenthesis immediately following the title.

4. **DESCRIPTIVE NOTES:** If appropriate, enter the type of report, e.g., interim, progress, summary, annual, or final. Give the inclusive dates when a specific reporting period is covered.

5. **AUTHOR(S):** Enter the name(s) of author(s) as shown on or in the report. Enter last name, first name, middle initial. If military, show rank and branch of service. The name of the principal author is an absolute minimum requirement.

6. **REPORT DATE:** Enter the date of the report as day, month, year, or month, year. If more than one date appears on the report, use date of publication.

7a. **TOTAL NUMBER OF PAGES:** The total page count should follow normal pagination procedures, i.e., enter the number of pages containing information.

7b. **NUMBER OF REFERENCES:** Enter the total number of references cited in the report.

8a. **CONTRACT OR GRANT NUMBER:** If appropriate, enter the applicable number of the contract or grant under which the report was written.

8b, 8c, & 8d. **PROJECT NUMBER:** Enter the appropriate military department identification, such as project number, subproject number, system numbers, task number, etc.

9a. **ORIGINATOR'S REPORT NUMBER(S):** Enter the official report number by which the document will be identified and controlled by the originating activity. This number must be unique to this report.

9b. **OTHER REPORT NUMBER(S):** If the report has been assigned any other report numbers (*either by the originator or by the sponsor*), also enter this number(s).

10. **AVAILABILITY/LIMITATION NOTICES:** Enter any limitations on further dissemination of the report, other than those

imposed by security classification, using standard statements such as:

- (1) "Qualified requesters may obtain copies of this report from DDC."
- (2) "Foreign announcement and dissemination of this report by DDC is not authorized."
- (3) "U. S. Government agencies may obtain copies of this report directly from DDC. Other qualified DDC users shall request through _____."
- (4) "U. S. military agencies may obtain copies of this report directly from DDC. Other qualified users shall request through _____."
- (5) "All distribution of this report is controlled. Qualified DDC users shall request through _____."

If the report has been furnished to the Office of Technical Services, Department of Commerce, for sale to the public, indicate this fact and enter the price, if known.

11. **SUPPLEMENTARY NOTES:** Use for additional explanatory notes.

12. **SPONSORING MILITARY ACTIVITY:** Enter the name of the departmental project office or laboratory sponsoring (*paying for*) the research and development. Include address.

13. **ABSTRACT:** Enter an abstract giving a brief and factual summary of the document indicative of the report, even though it may also appear elsewhere in the body of the technical report. If additional space is required, a continuation sheet shall be attached.

It is highly desirable that the abstract of classified reports be unclassified. Each paragraph of the abstract shall end with an indication of the military security classification of the information in the paragraph, represented as (TS), (S), (C), or (U).

There is no limitation on the length of the abstract. However, the suggested length is from 150 to 225 words.

14. **KEY WORDS:** Key words are technically meaningful terms or short phrases that characterize a report and may be used as index entries for cataloging the report. Key words must be selected so that no security classification is required. Identifiers, such as equipment model designation, trade name, military project code name, geographic location, may be used as key words but will be followed by an indication of technical context. The assignment of links, rules, and weights is optional.